

First cycle degree

**FUNDAMENTALS IN NUCLEAR PHYSICS**  
**2015-2016**  
**EXPERIMENTS**

**Ionel Lazanu, Oana Ristea, Alexandru Jipa, Mihaela Sin, Octavian Sima,**  
Marius Călin, Ovidiu Teșileanu

# **1. Dosimetry and Radiation Safety**

## Dosimetry and Radiation Safety

### Quantities and Units

Below follows a description of some basic quantities and units used when describing the effects of radiation on humans.

The **Activity** ( $A$ ) of a radioactive source is the number of the nuclear decays in the source per unit time. The SI unit for activity is *Becquerel* ( $Bq$ ).  $1 Bq = 1 \text{ decay/s}$ . The old unit is *Curie* ( $Ci$ ).  $1 Ci$  correspond to the activity of one gram of radium.  $1 Ci = 3.7 \times 10^{10} Bq$ .

The **Absorbed Dose** ( $D$ ) is the absorbed radiation energy per unit mass of material (for example a human body). The SI unit is *Gray* ( $Gy$ ).  $1 Gy = 1 J/kg$ .

**Dose Equivalent** ( $H$ ) (also referred to as *human-equivalent dose* or *radiation weighted dose*) is used in order to estimate the effect of a certain type of radiation on a biological system. Dose Equivalent is a product of the Absorbed Dose ( $D$ ) and the radiation weighting factor ( $W_R$ ) of the radiation type  $R$ .  $H = D \cdot W_R$ . If the total dose is an effect of more than one type of radiation, all contributions are added:

$$H = \sum_R D_R \cdot W_R$$

where  $D_R$  is the absorbed dose from a specific radiation type  $R$ . The SI Unit of the dose equivalent is Sievert ( $Sv$ ). The old unit is *roentgen equivalent in rem*.  $1 rem = 0.01 Sv$ .

The **Radiation Weighting Factor** ( $W_R$ ) gives a measure of the biological damage to a human for a particular type of radiation. Calculated values of  $W_R$  for various radiation types (and energies) are listed in table 1. We should note that  $W_R$  is dimensionless. This means that *Sievert* has the same dimension ( $J/kg$ ) as *Gray*. Since the unit *Sievert* should not be confused with the unit *Gray*, it might be clearer to speak of *Sievert* ( $Sv$ ) in terms of "equivalent  $J / kg$ ".

Table 1: Radiation Weighting Factors ( $W_R$ ) of for different radiation types.

Radiation Type	Energies	$W_R$
X-ray photons, $\gamma$ photons, electrons	All energies	1
protons	> 2 MeV	5
neutrons	< 10 keV	5
	10 keV – 100 keV	10
	100 keV – 2 MeV	20
	2 MeV – 20 MeV	10
	> 20 MeV	5
$\alpha$ , heavy ions, fission fragments		20

The *effective human-equivalent dose*, usually referred to as the **Effective Dose** is denoted  $H_E$ , and measures the whole-body biological damage due to various forms of radiation exposure of different parts of the body. This effective equivalent dose is given as follows:

$$H_E = \sum_T H_T \cdot W_T$$

where  $H_T$  is the dose equivalent for the tissue or body part  $T$ , and  $W_T$  is the tissue weighting factor for  $T$ .  $W_T$  is without dimension, so the unit of  $H_E$  is Sievert (Sv), the same as for  $H_T$ .

Values of **Tissue Weighting Factor** ( $W_T$ ) for different organs are listed in Table 2.

Tissue or Body Part	$W_T$
Gonads	0.20
Bone Marrow	0.12
Colon	0.12
Lung	0.12
Stomach	0.12
Bladder	0.05
Breast	0.05
Liver	0.05
Esophagus	0.05
Thyroid	0.05
Skin	0.01
Bone Surface	0.01
Remainder: adrenals, brain, upper large intestine, small intestine, kidney, muscle, pancreas, spleen, thymus, uterus	0.05
Total:	1.00

The dose rate distribution during exposure from a radioactive source depends on the types of ionising radiation emitted from the source and their respective energy release rates in the human body (*supposed as water*). For photons we estimate the dose rate from the photon energy flux and the photon mass energy-absorption coefficient  $\frac{\mu_{en}}{\rho}$ , see fig. 1.

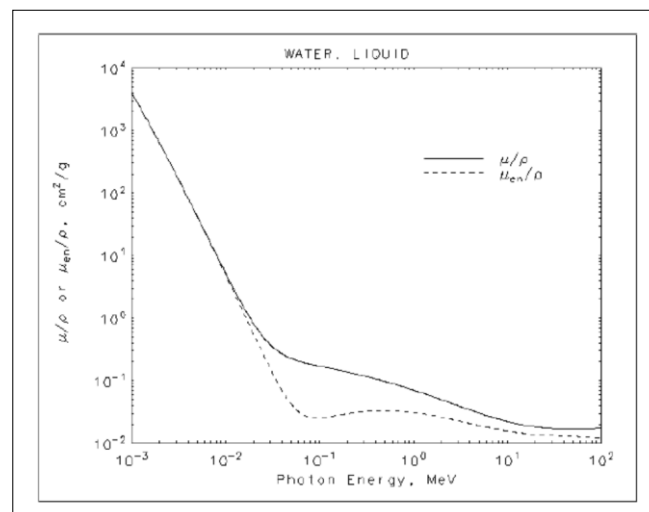


**Figure 1:** Values of the mass attenuation coefficient, and the mass energy absorption coefficient,  $\mu_{en}/\rho$ , in water as a function of photon energy. From the Nat. Inst. of Standards & Technology, <http://physics.nist.gov/>.

## Effects of Radiation on the Human Body

The effects of ionising radiation on the human body can be divided into two types; *deterministic effects* and *stochastic effects*.

### Deterministic Effects

A deterministic effect *will* appear as a consequence of a certain radiation dose, and will increase if the dose is increased. Deterministic effects will only appear after the absorption of high doses, and will usually show up shortly (within hours or days) after the irradiation. The deterministic effects include nausea, hair loss, damage to the blood and bone marrow, damage to the intestines, and damage to the central nervous system. The threshold level above which deterministic effects occur lies at 0.1-1 Sv. These first effects include temporary sterility and induced defects on embryos during early pregnancy. At a dose of 1-2 Sv the symptoms include nausea and vomiting (radiation sickness), effects on the blood, and bone marrow damage. At these dose levels, the majority of irradiated persons will recover to normal health within a few weeks. At higher dose levels, the damage of the blood and bone marrow will be increasingly severe. The dose level at which 50% of the irradiated persons will die within a certain time (usually chosen as 60 days) is called *median Lethal Dose (LD50)* and lies at around 4 Sv. At doses above 5 Sv, damages on the intestines will be considerable, and at even higher doses the central nervous system will be affected. Very few people have survived a full-body dose above 6 Sv. All of the above assume that the dose in question is absorbed in a short period of time (at a dose rate of 1 Sv/min or more). If the dose is absorbed at a low rate, the body is more capable to recover.

It should be pointed out that the dose levels at which deterministic effects occur are extremely high. A dose of 1 Sv is about 250 times higher than the average dose a person living in Sweden will absorb in one year.

### Stochastic Effects

A stochastic effect will only appear with a certain probability, after a certain dose has been absorbed. If the dose is increased, the probability for the effect will increase, but the effect itself will not be more severe. Stochastic effects can show up a long time (several years) after the exposure to radiation. The effects include various types of cancer, and genetic effects.

The stochastic effects are consequences of cell mutations (in contrast to cell death for deterministic effects). Such mutations could induce cancer or, if they appear in gametes, give effects on later generations. It is a difficult task to find the probabilities that govern the stochastic effects. One reason for this difficulty is that the dose is usually not known with good accuracy. Another problem is that the probabilities involved are small. As a consequence of this, it is often difficult to separate the effects of radiation from the effects of other factors.

Example:

Consider a person who receives a dose of 10 mSv during an accident in a laboratory. According to modern research on stochastic effects, the risk of death in cancer due to radiation is considered to be 5%/Sv. In the present case, the risk of death in cancer is  $0.05 \cdot 0.01 = 0.05\%$ . This number should be compared with the risk, from other factors, of death in cancer, which is around 20% in some European states.

The problem of stochastic effects of radiation on humans is complex and difficult. One question often under debate, is whether or not there exists a threshold dose level, below which no stochastic effects appear.

## Radioactivity in Our Daily Life

To find out if a dose absorbed during work with radioactive material will considerably increase the total absorbed dose, we need to know to what extent naturally occurring radioactivity affects us. The average effective dose differs much after region or country. Most probably, around 45% of this average dose comes from radioactive radon gas in houses, due to natural concentrations of radioactive isotopes (mainly  $^{40}\text{K}$  and  $^{14}\text{C}$ ). Medical diagnostic procedures and treatments represent around 35%. Other contributions include natural radioactivity in food, cosmic radiation, work with radioactive materials, etc.

### Dose Limits

The maximum allowed doses from ionising radiation for people living in Romania. These dose threshold values depend on various circumstances. The sum dose from all human activities regarding ionising radiation to the general public may not exceed:

Limita dozei efective pentru populație este de **1 mSv/an**.

În situații speciale, CNCAN poate autoriza o limită superioară anuală de până la **5 mSv/an**, cu condiția

ca valoarea medie pe 5 ani consecutivi a dozei efective să nu depășească **1 mSv/an**.

Respectând limita de doză pentru populație mai avem următoarele limite de doză echivalentă:

- 1 mSv per year effective dose
- 15 mSv per year equivalent dose to the eye's lens
- 50 mSv per year equivalent skin dose (averaged per  $\text{cm}^2$ )

For a person working professionally with radioactive materials (in nuclear medicine, nuclear power, etc) the maximum allowed effective dose is different. An other limit of these dose are valid for students below 18 years of age who use radiation sources in their education.

### Open and Sealed Sources

The radioactive sources used in the student laboratory can be divided into two types; *sealed sources* and *open sources*.

### Experimental work

In all the following measurements try to use all available types of dosimeters.

- 1) Draw the map of the laboratory.
- 2) Measure the approximate doses and rates of the doses in the laboratory and identify the regions with maximum rates of doses.
- 3) Draw the contours of iso-rate of doses in the laboratory.
- 4) For the regions with maximum rates of doses estimate the absorbed doses during the work in the laboratory and compare the results with dose limits for persons working with ionizing radiation.
- 5) Verify the variation of the rates of dose as function of  $1/(\text{distance})^2$ .

Compare the results obtained with different types of dosimeters. Estimate the systematic differences in results and try to explain the cause.

### Safety Measures in the Student Laboratory

All students should follow the rules in the list below.

- Never eat, or beverages or smoke in the laboratory.

- Wash your hands after handling radioactive material.
- If you have any doubts or questions concerning radiation safety, ask the laboratory assistant for help.
- The activity of radioactive sources can vary many orders of magnitude. Make sure that you know the activity of the source you are using.
- It is good practice to calculate the approximate dose that a certain source will give you during the exercise.
- Make sure that you know if the source is open or sealed. Never touch an open source.
- Always try to keep the radiation dose you absorb As Low As Reasonably Achievable (ALARA). This means for example that you should not hold a source in your hand any longer than necessary. Use lead or other materials to shield the source if you can reduce your dose in that way.

### Questions

The following questions should be answered before attending any activity in the nuclear physics student lab.

- What is the approximate (order of magnitude) dose a student will absorb during a laboratory exercise of five hours. Make reasonable assumptions about the average distance to the radioactive source, etc.

Calculate for the following two cases:

- A sealed (1 mm plastic shield)  $10 \mu\text{Ci}$   $^{137}\text{Cs}$  source.  $^{137}\text{Cs}$  emits gamma rays with photon energies of 662 keV and a branching ratio of 85%.
- An open  $1 \mu\text{Ci}$  alpha source emitting 5 MeV alpha particles inside a vacuum container made of 5mm steel.

Compare your results with the dose rate from the background radiation you are exposed to in your daily life.



## Features

- Stand-alone electronic dosimeter with LCD display, large non-volatile memory and programmable alarm levels on doses and dose rate
- Ultra thin/compact – light weight – shockproof – low cost
- Measures the X/γ dose equivalent Hp(10) according to ICRU 39
- Meets the latest regulations regarding the EMI compatibility – CE type approval
- Keystone of complete unique operational dosimetry systems

## DOSICARD™ – DOSIMAN Electronic Personal Dosimeters in Credit Card Size

### Description

With its credit-card size, DOSICARD™ features the smallest electronic dosimeter available on the market.

It is also one of the most technologically advanced. It provides real time monitoring of the personal dose and dose rate. DOSICARD is the key element within a unique operational dosimetry system that can be tailored to your specific applications. DOSICARD addresses all workers exposed to a radiological risk in nuclear facilities, research and medical centers, and the nuclear industry. Therefore, it is of outstanding performance in the ALARA strategy of minimizing received doses.

The DOSICARD badge is your radiation surveyor. It keeps you informed in real time of the radiation rate, allowing immediate reaction in case of radiation occurrence, thus drastically reducing the exposure to nuclear radiation.

DOSICARD can also be part of a system: from nuclear laboratories of a few persons to nuclear facilities of several thousand workers, Dosemanager II and CARD Systems allow easy operation, and database management for efficient operational dosimetry monitoring.

DOSICARD can display either Sv or rem, selection being made by the user in Dosemanager II. DOSIMAN can be delivered with either Sv or rem display (factory set).



**DOSICARD – Efficient and easy-to-use**  
DOSICARD features a silicon detector, complete analog and digital circuitry, including a microcontroller with large non-volatile memory, a LCD display and audio and visual alarms.

Three touch buttons allow programming and display setup of the current dose, dose rate and cumulative doses per day/month/quarter/year/five years.


### Phone contact information

Benelux/Denmark (32) 2 481 85 30 • Canada 905-880-5373 • Central Europe +43 (0)2230 37000 • France (33) 1 39 48 52 00 • Germany (49) 6142 73620  
Japan 81-3-3500-0806 • Russia (7-495) 429-8577 • Sweden +46 18 14 83 00 • United Kingdom (44) 1235 838333 • United States (1) 202-238-2351

For other international representative offices, visit our web site: [www.canberra.com](http://www.canberra.com) or contact the CANBERRA U.S.A. office.

C36214 3/08 Printed in U.S.A.



	<p><b>FH 40 G Multi-Purpose Digital Survey Meter</b></p> <p>Thermo Scientific* FH 40 G's integrated design represents a versatile, user-friendly, hand-held radiation measurement system. Designed for many different radiation protection applications. The FH 40 G is a wide range digital survey meter, suitable for nearly all measurement tasks arising in radiation protection.</p>
	<ul style="list-style-type: none"> <li>▪ Rugged, waterproof and reliable with very simple operation</li> <li>▪ Versatile multipurpose meter and area monitor</li> <li>▪ For use with external detectors for portable and remote area monitoring applications (cable of up to 50m can be used)</li> <li>▪ Gamma meter with internal proportional counter tube</li> <li>▪ Internal detector and external probes of the FH 40 G are monitored simultaneously</li> <li>▪ No requirement for external probe or cable for gamma dose rate measurements</li> <li>▪ Upon connection of an external probe, the probe parameters are automatically read into the FH 40 G and the correct parameters are set</li> <li>▪ Separate alarms can be set by the user for both the internal and external detectors</li> <li>▪ Operational internal proportional detector and connected external detector</li> <li>▪ Serial infrared interface</li> <li>▪ Type tested by PTB (Germany) in Hx or H*(10)</li> <li>▪ Type tested for use by fire brigades</li>   <li>▪ Calibrated in "air kerma" or in the new ICRU-units "ambient dose equivalent"</li> <li>▪ Simultaneous operation of internal and external detectors, both both dose rate and remote dose rate readings</li> <li>▪ Configuration and data read out via PC</li> <li>▪ Storage of up to 256 data records</li> <li>▪ Waterproof (IP 67) and shock resistant</li> <li>▪ ADF mode (Advanced Digital Filter)</li> <li>▪ Clear, backlit LCD display</li> <li>▪ Data logging</li> <li>▪ Internal diagnostics ensure proper functioning of the detector(s) and the electronics</li> <li>▪ Designed to record up to 256 data points containing measurement number, date, time and dose rate at the internal detector and external detector, status, and barcode information.</li> </ul>

### Limite de doză pentru persoane expuse profesional

Limita dozei efective pentru o persoană expusă profesional este de **20 mSv/an**.

Respectând limita de doză pentru expus profesional mai avem următoarele limite de doză echiv

- **150 mSv/an** pentru cristalin;

- **500 mSv/an** pentru piele; limita se aplică pentru valoarea medie a dozei pe  $1\text{cm}^2$ , pe cea mai puternic iradiată zonă a pielii;
- **500 mSv/an** pentru extremități.

### **Limite de doză pentru populație**

Limita dozei efective pentru populație este de **1 mSv/an**.

În situații speciale, CNCAN poate autoriza o limită superioară anuală de până la **5 mSv/an**, cu condiția

ca valoarea medie pe 5 ani consecutivi a dozei efective să nu depășească **1 mSv/an**.

Respectând limita de doză pentru populație mai avem următoarele limite de doză echivalentă:

- **15 mSv/an** pentru cristalin;
- **50 mSv/an** pentru piele; limita se aplică pentru valoarea medie a dozei pe  $1\text{cm}^2$ , pe cea mai puternic iradiată zonă a pielii.

### **Limite de doză pentru persoane în curs de pregătire**

Limitele de doză pentru persoanele având vârsta sub 16 ani care, în timpul pregătirii lor sunt obligate să utilizeze surse de radiații, sunt cele prevăzute pentru populație. Limita dozei efective pentru persoanele având vârsta cuprinsă între 16 și 18 ani care, în timpul pregătirii lor, sunt obligate să utilizeze surse de radiații, este de **6 mSv/an**. Respectând limitele de doză specificate, sunt valabile și următoarele limite de doză echivalentă:

- **50 mSv/an** pentru cristalin;
- **150 mSv/an** pentru piele; limita se aplică pentru valoarea medie a dozei pe  $1\text{cm}^2$ , pe cea mai puternic iradiată zonă a pielii;
- **150 mSv/an** pentru extremități.

Limitele de doză pentru persoanele având vârsta de peste 18 ani care, în timpul pregătirii lor, sunt obligate să utilizeze surse de radiații, sunt cele prevăzute pentru personalul expus profesional.

*(Sursa limitelor de doză: Ordinul Președintelui CNCAN nr. 14/24.01.2000, și publicată în MO Partea I nr. 404bis/29.08.2000 - Norme fundamentale de securitate radiologică, Art.21, 22, 25, 26, 27, 28 și 29)*

**2. Stochastic nature of radioactive decay:  
investigation of Poisson and Gauss  
distributions**

## Stochastic nature of radioactive decay: investigation of Poisson and Gauss distributions

### Purpose

In this experiment you will observe the random nature of radioactive decay, to do this we work on timescales much shorter than the half-life of the sample. Each radioactive decay event occurs independently of any other, so the measurement of the number of events detected in a given time period is never exact, but represents an average value with some uncertainty.

You will investigate uncertainties when counting randomly occurring events by investigating the decay of a radioactive source over different lengths of time. You will also study the relationship between the distribution recorded by a detector and the theoretical Poisson and Gaussian distributions.

### Theory

Radioactive decay is a stochastic phenomenon. It is impossible to predict *when* a radioactive atom will decay, only the *probability* for decay within a given period of time can be stated.

Pulse counting equipment for radioactivity measurements records a fraction of the radioactive decays in the sample within a given time period — this fraction is the counting efficiency ( $\epsilon$ ), and its magnitude depends on the radionuclide and the instrumentation used.

Since radioactive decay is a stochastic phenomenon, the same will apply for the number of pulses recorded from a radioactive sample within a given period of time — even if both the counting efficiency and the activity of the sample is assumed constant throughout this period. Thus, the recorded quantity (number of measured pulses  $\Delta M$  in a time period of length  $\Delta t$ ) is stochastic, and this will also apply for the derived counting rate,  $r = \Delta M/\Delta t$ .

That a measured quantity is stochastic means that it is impossible *in principle* to make exact quantitative predictions of the underlying phenomenon. *In this respect radioactivity measurements are different from most other physical measurements.*

Counting statistics in relation to radioactivity measurements deals with the statistical methods used to analyse and present primary measurement data and quantities derived from them.

The following must be taken into account:

- *The underlying phenomenon (radioactive decay) is a stochastic phenomenon. The activity of a radioactive sample therefore cannot be determined exactly, but it is possible to state the probability of the sample activity being within a given defined interval.*
- *The uncertainties and sources of variation associated with the measurement process - in principle of the same nature as for all physical measurements.*

Consider that  $N_0$  is the initial number of radioactive atoms (nuclei) at time  $t = 0$  (and a short time interval thereafter), and  $\lambda$  is the decay constant of the radionuclide, i.e. the probability of an arbitrary atom (nucleus) decaying during a time interval of unit length (e.g. 1 s).

Let  $\Delta N$  be the number of nuclear disintegrations occurring in a radioactive substance during a *finite time*  $\Delta t$ . According to the general law of radioactive decay,  $\Delta N$  may be written as

$$\Delta N = N_0(1 - e^{-\lambda\Delta t}) \quad (1)$$

The decay constant is non-stochastic quantity that is characteristic for the radionuclide in question. It is related to the physical half-life,  $T_{1/2}$ , by the expression

$$\lambda = \ln 2 / T_{1/2} \quad (2)$$

The decay constant is given in units of ‘reciprocal time’, e.g.  $s^{-1}$ ,  $\text{min}^{-1}$ ,  $\text{h}^{-1}$ .

The value of the decay constant for the various radionuclides are in principle associated with some uncertainty, since they are ultimately based on physical measurements. However, the experimental uncertainty is most cases small, and without practical significance for our purposes.

*Equation (1)* predicts an *exact value* for the number of nuclei disintegrating in any of a series of  $n$  successive time intervals, each of length  $\Delta t$ . The only precondition is that the total period of observation (from  $t = 0$  to  $t = \Delta t_1 + \Delta t_2 + \dots + \Delta t_n = n\Delta t$ ) must be short, so that the number of radioactive nuclei ( $N_0$ ) does not change significantly. In reality, this means that the period of observation must be short as compared to the half-life of the radionuclide ( $n\Delta t \ll T_{1/2}$ ).

In practice, however, the actual number of decays ( $\Delta N$ ) in the successive periods  $\Delta t$  turns out *not* to be constant; rather they scatter *around a mean value*. There may be different reasons for this, but the fundamental explanation is that radioactive decay is a *stochastic phenomenon*: each nucleus of a radionuclide has a well-defined probability of decaying during the time interval  $\Delta t$  (the probability may be expressed as  $\lambda\Delta t$ ), but it is impossible to predict exactly *when* a given nucleus will decay.

When repeating the determinations of  $\Delta N$ , the observed values will follow a *Poisson distribution* with a mean value predicted by *equation 1*.

Consequently, it does not make sense to state the value of  $\Delta N$  as a single number - that number must always be accompanied by an interval (around  $\Delta N$ ), within which the ‘true value’ is assumed to be with a given probability. *Equation 1* therefore does not predict an exact value, but instead the so-called *expectation value*, or ‘most probable value’ of the quantity in question. Or in an alternative formulation:  $\Delta N$  is a *stochastic physical quantity*.

## Relative and absolute measurements

As mentioned, only a fraction ( $\varepsilon$ ) of the disintegrations in the sample is normally recorded by the detector system. During the time interval  $\Delta t$ , a total of  $\Delta M$  counts (pulses) are recorded. The counting rate  $r = \Delta M / \Delta t$  is related to the disintegration rate  $\Delta N / \Delta t$  by the expression

$$r = \Delta M / \Delta t = \varepsilon \Delta N / \Delta t \quad (3)$$

where  $\varepsilon$  is the *counting efficiency* ( $0 < \varepsilon < 1$ ).

In general counting efficiency for the instrumentation used in laboratory is  $\varepsilon < 1$ . In other words, we normally rely on *relative counting* experiments.

Using symbols corresponding to *equation 1*, the absolute activity (the disintegration rate) may be written as  $dN/dt$ , cf. the differential form of the decay equation,  $dN/dt = -\lambda N$ .

## Measurement theory: True value, accuracy and precision

Any physical measurement may be considered an estimate of a ‘true’ or ‘theoretical’ value. When dealing with radioactivity measurements, the *true value* -  $\nu$ , may be equated with ‘the most probable number of counts (pulses) during the measurement period  $\Delta t$ . The true value is unknown *in principle*, but it is the objective of the measurement process to produce a result that may be taken as a measure of  $\nu$ .

The number of counts  $\Delta M$ , recorded in the period  $\Delta t$ , is taken as an estimate of  $\nu$ . Similarly, the count rate  $r = \Delta M/\Delta t$  is an estimate of the theoretical quantity  $\nu/\Delta t$ .

The terms *accuracy* and *precision* are often used to characterize the validity of experimental data.

The *accuracy* is a measure of the degree of proximity between the recorded result and the true value. The accuracy is high, if the results are close to the true value, which implies that significant systematic errors in the procedure

The *precision* measures the *reproducibility* of the measurements under identical conditions. If repeated measurements on the same sample produce close to identical results, the precision (reproducibility) is good.

It is possible for a given series of measurements to be characterized at the same time by a good precision and a bad accuracy. This means that the method reproduces results with little or no physical meaning! The concepts of accuracy and precision are illustrated in the following figure.

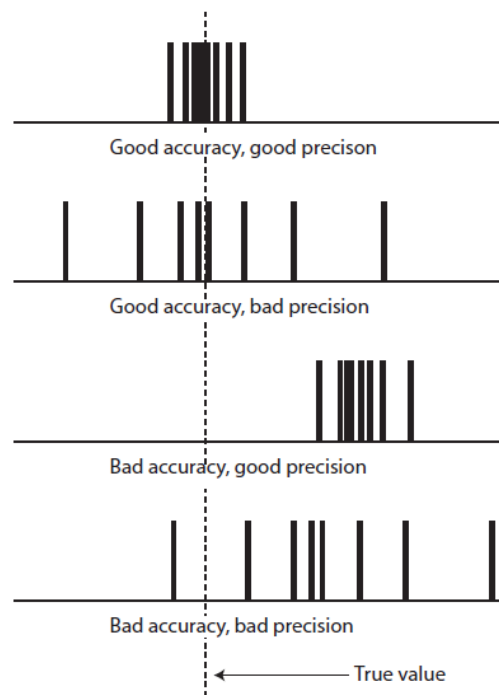


Figure: Illustration of the terms accuracy and precision. The distribution of results in four different combinations of good/bad accuracy and precision.

## Experiment

Random nuclear events follow a **Poisson distribution** that is the limiting case of the binomial distribution for an infinite number of time intervals, and closely resembles a Gaussian (or Normal) distribution if the mean is large. In the case of a large sampling size the probability  $P(N)$  that  $N$  pulses will be counted is a function of the expected number of pulses, which in this case can be replaced by the mean value  $\bar{N}$ ,

$$P(N) = \frac{\bar{N}^N}{N!} e^{-\bar{N}} \quad (1)$$

The Poisson distribution as given by Eq. (1) always describes radioactive decays irrespective of the value  $\bar{N}$ .

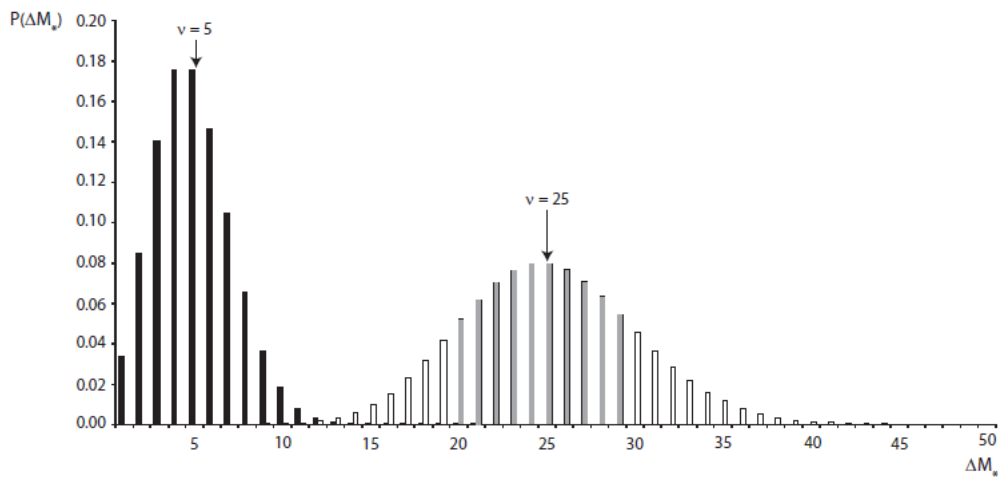
Such a distribution has a standard deviation, equal to the square root of  $\bar{N}$

$$\sigma = \sqrt{\bar{N}}, \quad (2)$$

For the cases where  $\bar{N}$  becomes large (exceed 25 for example), the Poisson distribution can be approximated to the **Gauss distribution**, defined as:

$$P(N) = \frac{1}{\sqrt{2\pi\sigma^2}} e^{\left[-\frac{(N-\bar{N})^2}{2\sigma^2}\right]} \quad (3)$$

As long as the standard deviation is defined by eq. 2 and account is taken of the discrete nature of the counts. The Gaussian distribution is always symmetric and bell shaped about the mean value, whereas the Poisson distribution is asymmetric if the mean value is small, i.e.  $\bar{N}$  is less than about 25.



Note that the general Gaussian distribution, Eq. (3), requires 2 parameters: the mean,  $\bar{N}$ , and standard deviation,  $\sigma$ , to describe it. In the Poisson distribution, Eq. (1) once  $\bar{N}$  is parameter.

### **Measurements**

This experiment uses a standard detection system with a scintillator detector (NaI(Tl)) and single channel analyser.

All the measurements will be registered using the following sequence (predefined in the installation): 10 sec. measurement, 2 sec. stop, reset the counter number of events, 10 sec. measurement, and repeat.

### **Background**

Start the measurements in the absence of radioactive source to obtain the value of the background of the installation (due to electronic circuits, cosmic rays, and the presence of different radioactive source in the laboratory).

Calculate the average value of the background using a set of 10 repeated measurements. This value will be  $\bar{b}$ .

### **Source**

Use a radioactive source with a very low activity to obtain a low count number for the decay processes. Suggestion for source: Co-60.

The number of  $x$  decay events of a radioactive preparation over a time interval  $\Delta t$  is not constant. A large number of individual measurements can be represented as a frequency distribution  $H(x)$  scattered around the mean value. By comparing this frequency distribution with the Poisson distribution, we can confirm that  $x$  shows a Poisson distribution around the mean value  $\mu$ .

In the evaluation, you can compare the measured frequency distribution with a Poisson distribution. For higher mean values the Poisson distribution develops into a Gaussian distribution.

Save your data and plot a histogram for every position of the source.

In the first position of the source the rate of events as (number of events/sec -  $\bar{b}/sec$ ) must be around the value 5-6.

In the second position this rate must be around the numbers 10-15, and in the last position this rate will be preferable more 25.

For every position the total number of repeated measurements must be at least 50.



### **3. Gamma – Ray Spectroscopy Using NaI(Tl) Detectors**

## Gamma – Ray Spectroscopy Using NaI(Tl) Detectors

### Purpose

In this experiment high energy photons - gamma-rays - are detected using scintillation detectors read out by photomultipliers. The gamma-ray energy spectra for various radioactive sources are measured and the linearity of the detection apparatus and energy resolution are determined.

### *Step 1. Basic Identification in Electronic Measurement Systems*

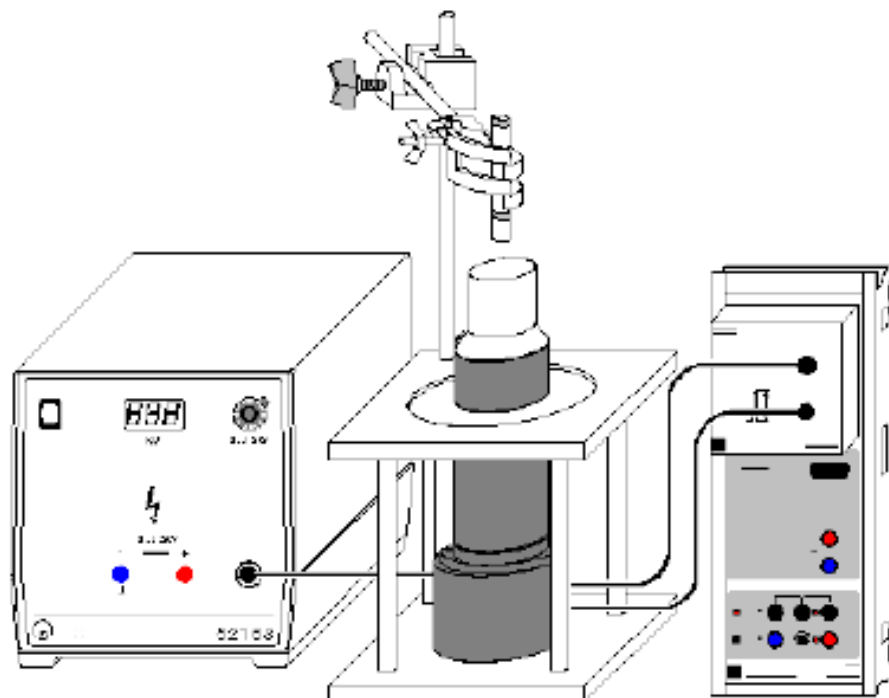
This set of exercises is intended to familiarize the students with basic electronic components that you will use to make subsequent measurements. Observe the signal at each stage and draw its shape, height (in volts), and length (in seconds). Alternatively, you can record the waveform using the appropriate oscilloscope function and plot the results.

### *Step 2. Gamma-Ray Spectroscopy Using NaI(Tl)*

Here you will use electronics from the first experiment to measure and analyze the energy spectrum deposited in a NaI(Tl) scintillation detector by gamma rays from different radioactive sources

### Experimental set-up

#### Recording and calibrating a $\gamma$ spectrum



### Experiment setup (see drawing)

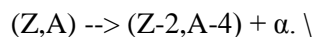
The output signal of the scintillation counter is connected to the MCA box and the high-voltage power supply. The preparation to be studied is placed few centimetres above the scintillation counter and it is fixed with stand material. In order to prevent the scintillation counter from toppling over, it is recommended to use the socket (559 891) for the setup.

## Radioactive Sources

### Nuclear Decay Processes

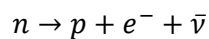
Radioactive nuclei can undergo a variety of processes with the emission of radiation. The three most important of these processes are: alpha decay, beta decay, and gamma emission. We briefly describe these processes below.

1. **Alpha decay:** It is the emission of an alpha particle (Helium nucleus) from the nucleus:

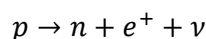


The emitted alpha particles are monoenergetic, with energy in the range of a few MeV. The alpha interacts strongly and has a very short range - a few cm in air.

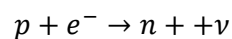
2. **Beta decay:** This is the decay of a neutron into a proton, electron and a neutrino:



The proton does not have enough energy to escape the nucleus but both the electron and neutrino do. The electron has a continuous energy spectrum because of the kinematics of the three body decay. A related process is the emission of a positron:



Other possibility is the electron capture:



Neither the electron nor the positron is very penetrating.

3. **Gamma emission:** The nucleus has discrete energy levels, like those of the electrons in an atom. The nuclear force, however, is much stronger than the electromagnetic and hence transitions from one state to the other are characterized by the emission of photons with much larger energy - from hundred keV to few MeV. Such photons are called gamma-rays and are very penetrating.

The probability that a nucleus will emit radiation is random and depends on the number of nuclei. Hence the mean number of decays as a function of time is given by the exponential:

$$N(t) = N(0) e^{-t/\tau}$$

where  $N(0)$  is the number of nuclei at  $t=0$ . The number  $\tau$ , is known as the mean lifetime - the time it takes the sample to decay to  $1/e$  of its initial activity. The half-life is the time it takes the sample to decay to one-half of its initial activity.

The activity of a source is the number of decays which can occur in a given time. It is usually measured in Curie who is defined as: 1 Curie =  $3.7 \times 10^{10}$  disintegrations/s.

This is a very large unit (originally defined as the activity of one gram of Radium). One usually deals with sources which have activities on the order of a microCurie ( $\mu\text{Ci}$ ).

In SI of units of measurements the activity is measured in Becquerel (1Bq=1disintegration/s).

The sources we use in this experiment have low activity. For example, a 100  $\mu\text{Ci}$   $^{22}\text{Na}$  source produces an exposure rate of 4.47 mrem/hr. For comparison, one x-ray produces a dose of 100-200 mrem. One rem is defined as energy of 100 erg deposited in one gram of material multiplied by a quality factor for the type of radiation. For gammas the quality factor is one. In SI units of measurements this quantity is Sievert. activity is measured in Becquerel ( $1\text{Sv}=1\text{J/kg}$ ).

### **Carrying out the experiment** Load settings

- Record the spectra of Co-60, and Na-22 (**F9**) one after another. It is recommendable to begin with the Co-60 preparation because the radiation it emits has the highest energy so that the high voltage and the gain can be adjusted appropriately from the very beginning.

- In order to get an energy spectrum, an energy calibration has to be carried out. For this the following lines will be used:

Co-60; the lines from transition at 1170 keV and 1330 keV

Na-22; line at 511 keV from positron annihilation and 1275 keV from gamma decay

### **Energy Calibration**

When a gamma ray (that is emitted during a change in an atom's nucleus) interacts with your sodium iodide crystal, NaI(Tl), the gamma will frequently give all its energy to an atomic electron via the photoelectric effect (photoeffect). This electron travels a short path in the crystal, converting its energy into photons of light by colliding with many atoms in the crystal. The more energy the gamma ray has, the more photons of light that are created.

The photomultiplier tube (PMT) converts each photon into a small current, and since the photons arrive at the PMT at about the same time, the individual currents combine to produce a larger current pulse.

This pulse is converted into a voltage pulse its size is proportion with the gamma ray's energy.

The voltage pulse is amplified and measured by an Analog to Digital Conversion (ADC) process. The result of this measurement is an integer between 0 and 1023 for a 10-bit ADC. Zero is the measure for a voltage pulse less than a hundredth of a volt, and 1023 is the measure for a pulse larger than about 8 volts (or the largest voltage pulse accepted by your ADC). Pulses between 0 V and 8 V are proportionately given an integer measure between 0 and 1023. This measure is called the channel number. The analog to digital conversion process is performed by your interface board. Your computer records and displays these measurements as the number of gamma rays observed for each integer measure, or channel number. Your screen displays the number of gamma rays as a function of the channel number.

Calibration with sources of known energies allows you to correlate the channel number with the gamma energy. The result is a graph of the gamma frequency (counts) as a function of gamma-ray energy (channel number). Figure 1 is a calibrated spectrum.

### **Suggested experimental procedure**

1. Connect the high voltage cable between the detector's PMT and the interface board.
2. Connect the data cable from the interface board to the PMT.
3. Start the multichannel analyzer (MCA) program.
4. Set the high voltage around 750 V and the amplifier gains to 4 on the coarse control and about 1.5 on the fine. Turn on the high voltage power supply from the computer screen.
5. Set the counts full scale to the linear scale and the conversion gain to 4,096 channels.

6. Place the source near the crystal end of the detector. Take data by selecting the Acquire button (or box).

7. Increase the amplifier gain by multiples of 2 until your spectrum looks like that of Figure 1. Your first adjustments should be with the amplifier gain. If you need additional gain, you may need to adjust your HV (high voltage) from the manufacturer's specification in 25 V steps. A good work conditions correspond to a maximum energy value – for example sum value for  $^{22}\text{Na}$  at 4/5 of full 4096 channels.

8. It is necessary to locate the centroid of each peak. If you use the  $^{22}\text{Na}$  source, you will observe the 511 keV line, 1274.5 keV and probably summation line (1786 keV). The 511 keV photopeak is from one of two gammas emitted simultaneously in opposite directions when a positron ( $e^+$ ) annihilates an electron ( $e^-$ ). For  $^{60}\text{Co}$  source the main transitions are at 1173.2 keV and 1332.5 keV respectively.

The center of each peak will be located with the help of the MCA's software. Place a region of interest (ROI) around each peak with the Set button and the marker. Click on the Region button. The peak centroid will be displayed for the ROI selected by the marker.

9. Acquire a gamma spectrum for each commercial radioactive source that is available to you. Record a sketch of each spectrum. Record the centroid value of the channel number, the corresponding value of energy and FWHM of each photopeak.

10. Select 'energy calibrate' or use available software to draw fit with a linear curve fit, where x-axis is the channel of the photopeak as a function of corresponding energy (y axis). A point correspond to (channel, energy) = (0,0) is considered in the fit. Thus, a minimum of other two-point are necessary for calibration your data.

11. You may be given an unknown source. Acquire its gamma spectrum and record the photopeak energies. Using the calibration curve, and the channel positions of every photopeak determine the corresponding energies. Using Appendix, determine the element(s) and isotopic mass(es) of your unknown source. Compare your conclusion with accepted result. Discuss the possible errors.

### Comments

With a ruler observe the energy range where the data follow mostly a linear relationship, and the region where they do not. If this is the real case, thus only a linear fit is not correct for all range of energies and a quadratic fit of the data is required. Compute the quadratic fit to your data with a least squares fitting routine and verify the goodness of these new results. Attention: for a linear fit are necessary a minimum of 3 points, for the quadratic fit a minimum of four points are required.

Use the mixed source and identify the isotope using the catalog for isotopes.

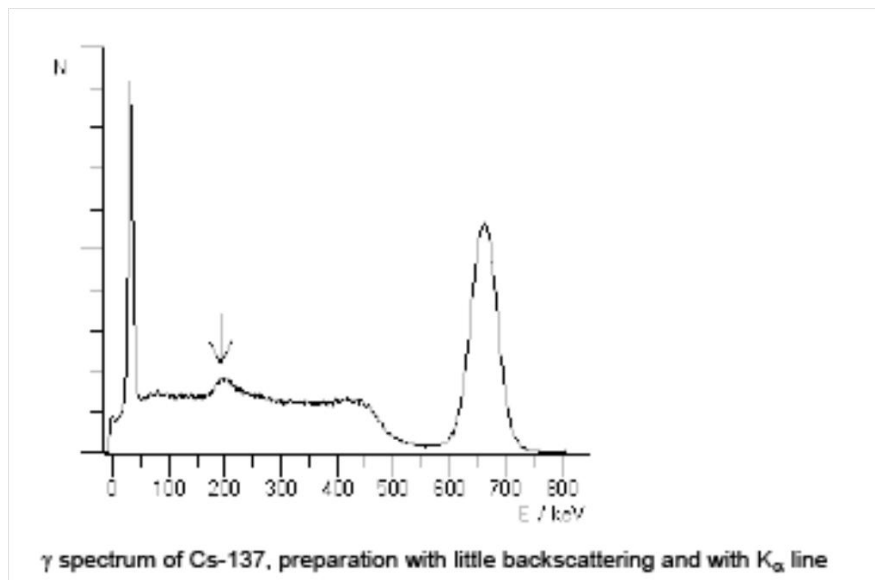
**Caesium-137** is a man-made radioactive isotope with a half-life of 32 years. It decays via  $\beta$  decay into barium-137. Of these decays 94.6 % lead to a metastable excited state of barium, Ba-137 m, which passes into the ground state with a half-life of 156 s, whereby a  $\gamma$  quantum of 661.6 keV is emitted. The remaining 5.4 % lead directly to the ground state of barium. The maximum energies of the emitted electrons are 513.97 keV and 1175.6 keV.

Emission of a 661.6 keV  $\gamma$  quantum is not the only way metastable barium gives off its energy. In other cases it can transfer its energy to an electron of the 1s shell of its atomic shell ("internal conversion"). The electrons than have an energy of 625.67 keV, that is the difference between the excitation energy of barium and the electron's binding energy. in contrast to beta decay, there is no continuum of the electron energy because no third particle is involved. The hole in the 1s shell is replenished from higher shells. This process gives rise to emission of the characteristic X radiation of barium, particularly of the  $K\alpha$  line at 32.19

keV. Because of the monoenergetic  $\gamma$  line at 661.6 keV, this isotope is well suited for studying the Compton effect and for energy calibration.

Depending on the cover of the preparation, the  $K\alpha$  conversion line at 32.19 keV is also visible and can be used for energy calibration, too. The Cs/Ba-137 isotope generator (559 815) contains Cs-137 as a salt from which Ba-137 can be washed out. Because of the low mass of the covering plastic housing, this source exhibits a distinct line at 32.19 keV and a very weak backscatter peak even without wash-ing the barium out.

The mixed preparation (559 84) exhibits a distinct backscatter peak because of the aluminium holder but no  $K\alpha$  conversion line.



### Detector Energy Resolution

Statistical processes in the detection system cause the large width observed in the gamma peaks. The conversion of a gamma's energy into light, and the collection and conversion of that light into an electrical pulse, involve processes that fluctuate statistically. Two identical gammas, fully-absorbed in the crystal, may not produce exactly the same number of visible photons detected by the PMT. Equal numbers and energies of visible photons will not produce the same number of electrons at the PMT output. These electrical pulses from the PMT have different pulse heights even though they represent the same gamma energy. The result of these statistical processes is a distribution of pulse heights that can be represented by a normal or Gaussian distribution curve, shown in Figure 1.

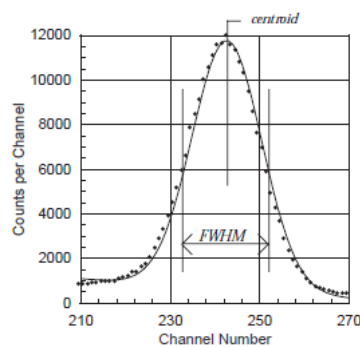


**Figure 1.** Photopick and gaussian fit to the 511 keV gamma line from a  $^{22}\text{Na}$  spectrum

The resolution is the ratio of some measure of the width to the centroid value, which provides a succinct number to describe this width. It is standard practice to use the Full-Energy Width

at Half the Maximum peak count (FWHM) above the background as the measure of the photopeak width. This is proportional to the standard deviation of the distribution's average value (centroid). The ratio of the FWHM to the photopeak energy is a dimensionless quantity called the fractional energy resolution,  $\Delta E/E$ .

$$N(E) = \frac{N_0}{\sqrt{2\pi\sigma^2}} e^{-\left(\frac{(E-E_m)^2}{2\sigma^2}\right)}$$

This is the equation for the normal (Gaussian) distribution with a peak area of  $N_0$ . The average energy is  $E_m$  and  $\sigma$  is the standard deviation of that average. The FWHM = 2.3548  $\sigma$ .

From purely statistical arguments, it can be shown that  $\frac{\Delta E}{E} \propto \frac{\sqrt{E}}{E}$ . Experiment and theory for NaI(Tl) detectors have shown us that we can represent this proportionality as  $\left(\frac{\sqrt{E}}{E}\right)^2 = \frac{m}{E} + b$  where m and b are constants that could be determined.

**Comment** The overlapping spectra between two or more photopeaks is a typical difficulty in spectroscopy. The finite width of the observed photopeak implies that it is difficult to measure the center of each of two photopeaks if their gamma energies are separated by something less than the photopeak widths. Figure 2 is an example of the effect of different resolutions upon a spectrum of two gamma photopeaks.

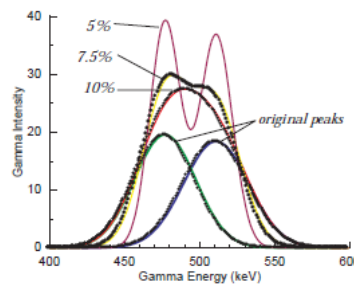


**Figure.2** The overlapping spectra above are of two equal area photopeaks centered at 477 keV and 511 keV. The individual photopeaks are shown at 10% resolution underneath the other spectra.

The combination of the two photopeaks is shown for resolutions of 5%, 7.5%, and 10%.

At 5% resolution for each peak, the combined (added) spectrum from the two photopeaks is visibly resolved as two peaks. At 10% resolution the two peaks blend together as a single, broad peak. Obviously it is easier to determine the centers of the photopeaks when they are clearly resolved, as are the 5% peaks of Figure 2. Understanding the resolution of a detector and minimizing it is one of the driving forces behind research into new detectors.

### Suggested experimental procedure

1. Start the MCA and check the calibration using a gamma source from laboratory. The observed photopeak should be centered near the theoretical value. If the system is correct calibrated, thus the experimental value is not within 10keV of the accepted value, in the contrary case you may need to recalibrate your system.
2. Select a Region Of Interest (ROI) around your photopeak. Record the centroid of the photopeak and its FWHM.
3. Repeat this step for all the sources available to you.

**Data Analysis**

From your data of photopeak energies and corresponding FWHM calculate the fractional resolution and graph its square as a function of the inverse of the corresponding photopeak energy. Use a linear least squares program to get the equation for the best straight line fit to your data. Graph this equation on the graph with your data. Is your fit to the data a good fit?



## Annexes

### 1) NaI(Tl) Scintillation Detectors

Gamma ray detection with a NaI(Tl) crystal was discovered by Robert Hofstadter in 1948. Since then the scintillation detectors (many different crystals present scintillation phenomena), in particular the NaI(Tl) detector, have been used in a wonderful array of important physical experiments. These experiments include the discovery of positronium ( $e^+$ ,  $e^-$  atom), mu-mesic atoms (an atom with an “orbiting”  $\mu^-$ ), Mossbauer spectroscopy, the Pound and Rebka gravitational redshift experiment, positron emission tomography (PET), and the discovery of the astronomical gamma ray bursts, to mention just a few.

The discovery of the NaI(Tl) scintillation detector was not accidental but came from a path of physical reasoning and good fortune. Scintillation was well known in the 19th century, and ZnS(Ag) crystals were used by Rutherford in his alpha-scattering experiments. Scintillators are known in gaseous, liquid, and crystalline forms, and the gamma-detecting scintillators, anthracene crystals and naphthalene crystals were developed prior to Hofstadter’s discovery of NaI(Tl). Hofstadter followed the technique used by Hartmut Kallmann with naphthalene, placing the scintillating material in front of a photomultiplier tube to detect any luminescence produced by gamma rays interacting with the crystal. Hofstadter’s good fortune was having in his possession an excellent KI(Tl) crystal produced a decade earlier by Frederick Seitz and Frank Quinlan at General Electric. He used this crystal because its density was greater than either anthracene or naphthalene crystals, which theoretically should result in a larger gamma-ray stopping power. This behaviour was indeed observed, but the electrical pulses from the photomultiplier were smaller than those produced by the naphthalene crystals under similar observational conditions.

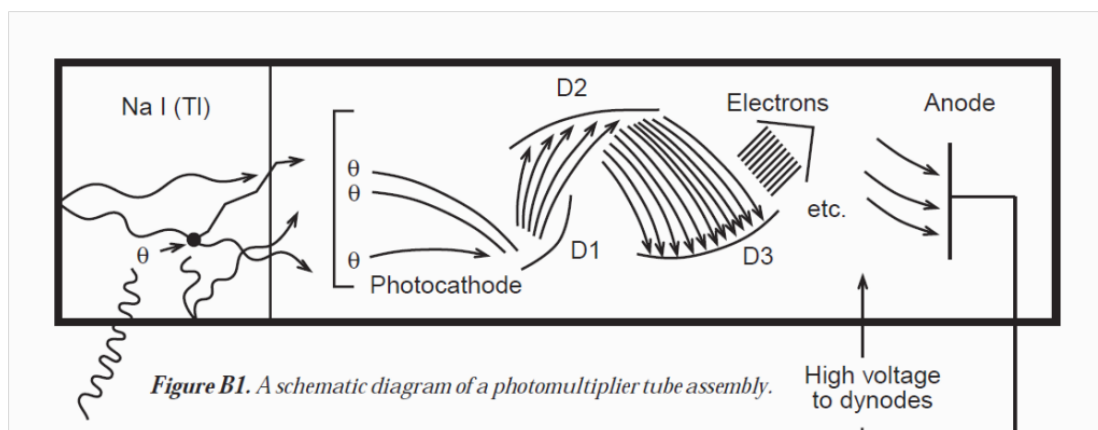
Hofstadter studied papers written by some German researchers on luminescence in alkali-halide crystals, and decided to study NaI because so little was known about it, and because it emitted light in a wavelength region that the crystal did not strongly self absorb and for which the photomultipliers were quite efficient at detecting. A comparative test of the scintillation of various crystals and powders demonstrated that the NaI(Tl) crystals were much more efficient than all the other crystals tested. With a small crystal (actually a polycrystalline sample) in a 1/2” test tube, Hofstadter observed large voltage pulses from a photomultiplier coupled to his crystal. Later that same year Hofstadter and McIntyre observed that the scintillation pulses were grouped into “lines”, revealing the spectroscopic abilities of the NaI(Tl) crystals. Their results, published in the Physical Review, showed the near linearity of the pulse heights with gamma energy from the spectra of known gamma-emitting isotopes. This led to the quick, world-wide spread of the use of the NaI(Tl) detector for nuclear-gamma spectroscopy.

### NAI(TL) SCINTILLATION

Gamma interactions with matter eventually produce electrons with kinetic energies whose sum is equal to the energy of the original gamma. The interactions include the photoeffect, Compton scattering, and pair production. You have or will study these interactions in several of the experiments outlined in this book. How do the electrons created in your NaI(Tl) crystal by a gamma eventually result in luminescence in the visible and ultraviolet? NaI is a nonconducting crystal, implying a large energy separation between its valence band and its empty conduction band. Energetic electrons produced by a gamma will dissipate their kinetic energy via the production of electron-hole pairs produced by collisions with electrons in the crystal. Recombination of these electron-hole pairs can result in light emission by radiative transitions or heating in the form of lattice vibrations. The presence of thallium at the  $10^{-3}$  molar fraction level significantly increases the light emission of the crystal, and it is referred to as an activator for the crystal. Experiments have shown that luminescence from the activated NaI(Tl) crystals is characteristic of an excited state decay in thallium ions ( $Tl^+$ ), even though the energy of the gamma (and the electrons that it produced) is dissipated almost entirely in the NaI host! The diffusion rates of the electrons and the holes (they are not the same) result in thallium emission that decays nearly exponentially after the first few

microseconds. Almost two thirds of all the luminescence is emitted in the first quarter of a microsecond. This time is important because to be useful as a detector of individual gamma photons, the flashes of light (scintillations) must be distinguishable in time. The production of electron-hole pairs from a gamma interaction usually takes less than a nanosecond and does not affect this result. The result of the Thallium activation of NaI is a crystal that converts about 11% of the incident gamma energy into photons with an average energy of 3.0 eV. The burst of photons has a characteristic (although not purely exponential) time of 0.23 msec with a maximum emission at wavelength of 415 nm. A 1,000 keV gamma will produce, on average,  $4.3 \times 10^4$  photons. Statistical variations in this number for each 1,000 keV gamma observed is one of the contributing factors in the observed width (energy resolution) of the photopeaks.

## PHOTOMULTIPLIERS



Rutherford and his graduate students used their eyes to detect the individual scintillations from their ZnS phosphor. Distinctions between variations of the light intensity of individual pulses is very difficult if not impossible. In the late 1930's a tube was invented that converted light into an electron current that was amplified by many orders of magnitude. This tube eventually became the television camera of the 1960's and 1970's and became the photomultiplier for observing the scintillations from NaI(Tl) and detecting of low intensities of light in general. A typical photomultiplier tube is shown in Figure B1. The photomultiplier has a semitransparent photocathode at its detecting end which produces with some probability, one electron for each photoelectric event, for photons between designed photon wavelength ranges. For NaI(Tl) scintillations, the wavelength range is centered near 415 nm. The photoelectron is accelerated between the photocathode and the first dynode, striking the dynode with a kinetic energy between a few tens and a hundred eV. The collision at the surface of the first dynode produces a few electrons for each incident electron. These electrons are accelerated to the second dynode where the process is repeated for each succeeding dynode until the last electrons are collected at the anode. The multiplications of the electrons can exceed a factor of a million for typical potential differences applied across the photocathode and anode of the PM tube. In general the multiplication factor increases with the magnitude of the applied potential difference, typically 700- 1,000 volts. Up to 20% of all the photons incident upon the PM tube produce an electron at the photocathode. Collection

efficiencies by the first dynode and the anode can change depending upon the application and the applied potentials. Each individual dynode's potential is determined by dividing the potential difference between the photocathode and the anode with a resistor chain. This resistor chain is usually located in the detachable base of the PM tube, and can be reconfigured. Some resistors are variable to allow external adjustment of one or more potentials, usually the focusing (photocathode to first anode potential difference). The PM tube supplied with your Spectrum Technique's MCA board is factory set for the best

operating conditions over a reasonable range of applied potential differences, about 500-1,000 volts. There is a finite amount of time for the initial photon pulse to be converted into an electrical charge at the anode. Increases in the decay time of the incoming pulse are minimized so that the output pulse from the PM tube is about the same as the input pulse.

### **NaI(TL) DETECTOR**

The pulse height resolution of the detection system depends upon collecting as many as possible of the photons created by the incident gamma ray as possible. The photons emitted by the thallium ions are emitted in all directions, so a high efficiency reflector,  $\text{Al}_2\text{O}_3$  and Teflon are used around the scintillator to reflect as much light as possible into the PM tube. The air gap between the scintillator and the PM tube can result in significant losses due to reflections and non normal angles. This is minimized by filling the air gap with a silicon grease with an index of refraction intermediate between that of the crystal and the glass of the PM tube. Magnetic fields originating externally to the PM tube, can profoundly change (decrease) the multiplication factor. Enclosing the PM tube (except for the entrance window) in a magnetic shield is very important. The entire detector is enclosed in an aluminum case to prevent light leakage into the PM tube.

## **2) ELECTRONICS**

The charge collected on the anode from one scintillation pulse is still quite small. A preamplifier (in the PM base or external to the base) that drains the charge collected on the capacitance between the anode and the preamp is used to convert the output pulse from the anode into a voltage pulse with a decay time of  $R_p C_p$ .  $R_p$  and  $C_p$  are the feed back resistance and capacitance of the preamps high gain, inverting amplifier. The preamp acts as a low impedance source of voltage pulses. The output voltage of the preamp is proportional to the total charge transferred from the anode to the preamp's input. The preamplifier output is usually only a few tenths of a volt and must be further amplified to use as much of the multichannel analyzer's typical 0-8 volts input on the analog-to-digital converter. Most amps used for this purpose are AC coupled, introducing another time constant to the decay of the voltage pulse. The time constant is adjusted to achieve the best pulse height resolution. AC coupling requires that the integrated voltage pulse is zero, resulting in overshoot. Base-line restoring electronically prevents a succeeding pulse from adding to the overshoot, essentially reducing its pulse height. The preamp and the amplifier have been set on your Spectrum Technologies detector and amplifier so that you need only select the operating voltage for the PM tube and the amplifier gain in software.

**Preamplifier** - The preamplifier converts the pulse from the photomultiplier anode - a charge pulse - to a voltage pulse using a capacitor. The rise time of the pulse (important for timing measurements) is dependent upon the scintillation decay time and on the collection and transit time characteristics of the photomultiplier tube.

**Amplifier** - Besides amplifying the pulse this unit shapes the pulse to obtain either optimum energy resolution or time resolution. Observe the effect of the different pulse shape controls (differentiation and integration switches). Note that the decay time of the pulse is much shorter than after the preamp. This is done to prevent overlap (pile-up) of pulses in a high count rate experiment.

**Single Channel Analyzer** - This instrument produces a logic output pulse indicating the presence of a linear input pulse within the range determined by the "E" and "E+ $\Delta E$ " settings (differential mode) or merely exceeding the "E" setting (Integral mode). Also, the logic output

pulse bears a definite time relationship to the linear pulse causing it. Thus this module converts linear signals to logic signals used in the time coincidence experiment.

**Multi-Channel Analyzer** - This versatile instrument gives a plot of the pulse height spectrum of all of the pulses input to it. It takes each pulse, converts its pulse height into a digital number and increments the bin count that number falls within.

## **4. Measuring the activity of a radioactive source**

## Measuring the activity of a radioactive source

### The activity measurement

The activity  $A$  of a radioactive source with  $N$  nuclei of a certain species is defined as the number of decays per unit time

$$A = -dN/dt = \lambda N \quad (1)$$

where  $\lambda$  is the decay constant and  $dN$  is the variation of the number of nuclei of that species due only to decays. The experimental activity determination can be made by recording the photon detection rate  $R_{\text{peak}}$  (number of photons detected per time unit) due to a particular transition with **branching ratio**  $B_R$ . If the detection efficiency for these photons is  $\varepsilon$ , the source activity is given by:

$$A = R_{\text{peak}} / \varepsilon B_R \quad (2)$$

The *total efficiency*  $\varepsilon$  can be factorized into two terms: *geometric acceptance* or *geometric factor* and *detector intrinsic peak efficiency*.

### About NaI(Tl) scintillator as radiation detector

The NaI(Tl) gamma detector is widely used in laboratories of radiation physics. This type of detector can be used to measure radioactive sources activities, providing the detector efficiency is known. The activity measurement by an absolute method is a highly pedagogic experiment, where experimental uncertainties must be under control in order to achieve a meaningful result. The main problems can be grouped into three categories: a) geometric acceptance, b) detector efficiency and c) data analysis.

The geometric acceptance should in principle be possible to compute if the source, detector and set-up dimensions are accurately known. For radioactive sources with finite dimensions the problem can become somehow mathematically complex. In what concerns the detector intrinsic efficiency, reliable data is not usually provided by the detectors manufacture, leaving the potential user the task to measure it with calibrated radioactive sources, or to compute it. The first option is not always possible in a teaching laboratory since calibrated radioactive sources are expensive and several calibrated sources with different energy peaks should be available in order to cover some energy range. Computing the detector efficiencies looks thus very attractive.

### Definitions of various parameters

#### 1 Efficiency

**1.1** The *intrinsic total efficiency* is defined as the ratio of the total number of events which are detected to the total number of  $\gamma$ -ray photons incident on the detector.

This number is determined by different factors: a) the existence of shielding materials which surround the scintillator; b) are geometric effects: if  $\gamma$ -rays are incident along the side of the cylindrical scintillator, then the path length varies with incident location. For sources at a large distance, this is a small correction, but if the distance to the source is less than 20 times the detector dimension, then the correction may be quite important; c) it is possible for the signal processing electronics to fail to detect an interacting  $\gamma$ -ray, when the amplitude of the pulse is very small, below the noise threshold of the electronics; d) the losses of signals due to dead time of the electronic at sufficiently high count rates.

**1.2** The *photofraction* is defined as the ratio of the number of events which deposit their full energy in the detector, forming the photo-peak, to the total number of events which are detected.

Photopeak counts are produced by photoelectric interactions or if the incident  $\gamma$ -ray is scattered and the secondary particle is stopped in the detector. The photofraction increases for larger detectors, as more secondaries are captured. It depends on the geometry of the detector and also on the distance to the source.

**1.3** The *intrinsic photopeak efficiency* is the ratio of the number of full energy events to the total number of  $\gamma$ -ray photons incident on the detector. It is the product of the *intrinsic total efficiency* and the *photofraction*.

**1.4** The *absolute total efficiency* is defined as the ratio of the total number of events which are detected to the total number of  $\gamma$ -ray photons emitted by the radioactive source. It is the *product of intrinsic total efficiency and a geometric factor*  $G_F$ , (see definitions 1.1 and 2.) which yields the fraction of the emitted  $\gamma$ -rays which are incident on the detector.

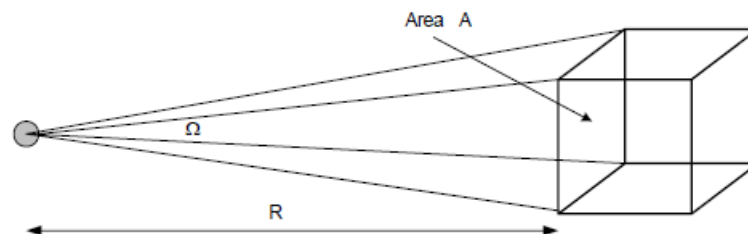
**1.5** The *absolute photopeak efficiency* is defined as the ratio of full energy events to the total number of  $\gamma$ -ray photons emitted by the radioactive source. It is the product of absolute total efficiency and photofraction.

**1.6** The *relative efficiency* is defined as a ratio between efficiencies of different detectors in the same geometry and under the same conditions. As standard detector is considered a 3"x3" NaI(Tl) scintillator at 1332 keV. The relative efficiency may certainly be >100% in this definition (!).

## 2 The geometric acceptance (geometric factor)

A source is located at a distance  $R$  from a detector with the area  $A$  facing the source. The  $\gamma$ -rays are emitted isotropically, i.e. with equal probability in all directions, with solid angle  $4\pi$  steradians. Seen from the source, the detector subtends a solid angle  $\Omega$ , defined by the area of the detector, which determines the geometric factor. At a large distance, the fractional solid angle is just the area  $A$  divided by the area of a sphere with radius  $R$ , and this is the fraction of  $\gamma$ -rays incident on the detector.

A simple formula holds if the separation between the source and detector is large. See the figure:



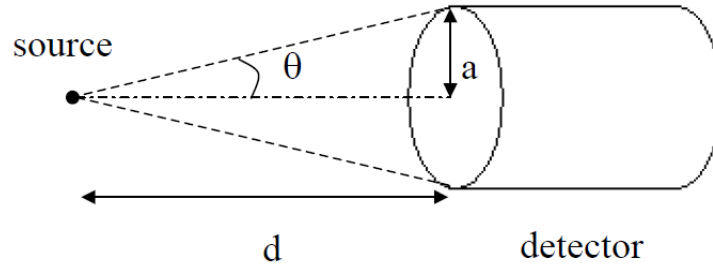
Thus,

$$G_F = \frac{A}{4\pi R^2}$$

If we consider the limit of small separation, the detector subtends half the solid angle, and this does not change even if the source is moved slightly away from the detector. For intermediate

values, analytical approximations have been computed for a variety of different geometries. A possible configuration is presented bellow:

For a cylindrical detector, solid angle seen by a point source place at a distance  $d$  is presented in the figure



and the geometrical factor is calculated as:

$$G_F \equiv \varepsilon_G = \frac{1}{4\pi} \int d\Omega = \frac{1}{4\pi} \int_A \frac{\vec{r} \cdot \vec{n}}{r^3} dA$$

$$\Delta\Omega = \int_0^{2\pi} d\phi \int_{\cos\theta}^1 (\cos\theta') = 2\pi(1 - \cos\theta)$$

where

$$\tan\theta = \frac{a}{d}$$

$$\cos\theta = \frac{1}{\sqrt{\tan^2\theta + 1}} = \frac{d}{\sqrt{a^2 + d^2}}$$

$$G_F \equiv \varepsilon_G = \frac{\Delta\Omega}{4\pi} = \frac{1}{2} \left( 1 - \frac{d}{\sqrt{a^2 + d^2}} \right)$$

If  $d \gg a$ , thus,  $G_F \cong \left(\frac{a}{d}\right)^2$ .

### Experimental Steps

Use a source located at 50cm in front of a cylindrical NaI(Tl) scintillator with knowed dimensions. For experiment use  $^{137}\text{Cs}$  source for example. Time for background measurement is 10 minutes and for measurent with radioactive source is  $t=100$  sec.

The activity of the source is  $A$  (unknown). This activity correspond to a number of disintegrations per second ( $1 \mu\text{Ci} \equiv 37 \text{ kBq} = 3.7 \times 10^4$  disintegrations per second).

- From this number of disintegrations, only a fraction is emitted as  $\gamma$ -ray of interest; the measure is the branching ratio ( $B_R$ ) This information will be extracted from the tables of isotopes. Thus,  $\gamma$ -rays per second emitted by the source is  $(AB_R)$ .

- Calculate the geometric factor  $G_F$  for the experimental setup. Thus, the fraction of emitted  $\gamma$ -rays which are incident on the detector is represented by the quantity ( $R_{inc} = AB_R G_F$ ).

- The total intrinsic efficiency of the detector will be obtained from the diagram. This is

$\varepsilon_{\text{intrinsic}}$  (Fig. 4).

- The photofraction (photopick ratio) will be obtained also from the diagram. This is

$\varepsilon_{\text{photofraction}}$ .

From these we can compute the total rate of interactions  $R_{\text{tot}}$ , and the photopeak rate,  $R_{\text{peak}}$ .



$$R_{\text{tot}} = R_{\text{inc}} \cdot \epsilon_{\text{intrinsic}}$$

$$R_{\text{peak}} = R_{\text{tot}} \cdot \epsilon_{\text{photofraction}}$$

For these rates (as true values) must extracted the rate for background.

In fact, supplementary, must be considered additional contributions: the attenuation of  $\gamma$ -rays in air, source and detector, attenuation in the aluminum window of detector, well as well in other possible materials between source and scintillator crystal. The radiation beam  $I$  almost decrease exponentially as the thickness of layer  $d$  increases,  $I = I_0 e^{-\mu d}$ .

Finally, the activity of the source will be obtained.

$$R_{\text{peak}} = AB_R G_F \epsilon_{\text{intrinsic}} \epsilon_{\text{photofraction}}$$

$$A = \frac{R_{\text{peak}}}{B_R G_F \epsilon_{\text{intrinsic}} \epsilon_{\text{photofraction}}}$$

Energy [keV]	Distance (cm)	Peak integral	Geometrical factor (acceptance)	Peak efficiency	Activity ( $\mu\text{Ci}$ )

An important problem is: How well can we distinguish a source from background and random statistical fluctuations? How weak a source can be detected?

For a correct estimation, we define a region of interest (ROI) within the spectrum, photopick region for present case.

We define:

$N_B$  is the number of counts within the ROI due to background.

$N_S$  is the number of counts within the ROI due to the signal, the total area between the two curves, sometimes called net counts.

$N_T$  is the total number of counts within the ROI, sometimes called gross counts:

$$N_S = N_T - N_B$$

If there were no fluctuations in the counts or other source of uncertainty, then if  $N_S$  were greater than zero, we would conclude that a source was present, and if  $N_S$  were zero, we would conclude that no source is present.

But there will always be statistical fluctuations in the counts, due to the random nature of radioactive decays, and there are likely to be additional sources of uncertainty and fluctuation in a real instrument. We therefore must require that  $N_S$  be greater than zero by its uncertainty times factor  $k$ , which determines the confidence:

$$N_S \geq k(\sigma_{N_T})$$

We have

$$\sigma_{N_S}^2 = \sigma_{N_T}^2 + \sigma_{N_B}^2$$

and

$$\sigma_{N_T}^2 = N_T + N_S + N_B$$

so

$$\sigma_{N_S}^2 = (N_S + N_B) + \sigma_{N_B}^2$$

⇒

$$N_S^2 \geq k^2(N_S + N_B + \sigma_{N_B}^2)$$

This implies that  $N_S$  must exceed a value which depends on the background rate and on the uncertainty in the estimate of the background rate. There is some lower limit on the total counts, or for a fixed measurement time, on the count rate. For a given absolute efficiency, this implies a minimum activity.

The  $\sigma_{N_B}^2$  term arises because we do not directly measure the background in the ROI, we estimate it from something else. This term represents the uncertainty in the background estimate and so depends on the algorithm used to estimate the background. In the plot above, we used a prior measurement of the background to estimate  $N_B$ , but this is not always possible. A common alternative is to estimate it from the spectrum itself, for example using the thin gray line drawn across the ROI. The measured counts in channels just outside the ROI are then used to estimate  $N_B$ . These two algorithms will yield different values for  $\sigma_{N_B}^2$ .

### Scintillation Counter NaI (Leybold Didactic GmbH)

<b>Crystal:</b> Material: NaI(Tl) Diameter: 381 mm Thickness: 50.8 mm	<b>Aperture:</b> Material: Aluminum Thickness: 0.4 mm Grounding: 190 mg cm <sup>-2</sup>
--	---

### Absolute total efficiency for NaI crystals

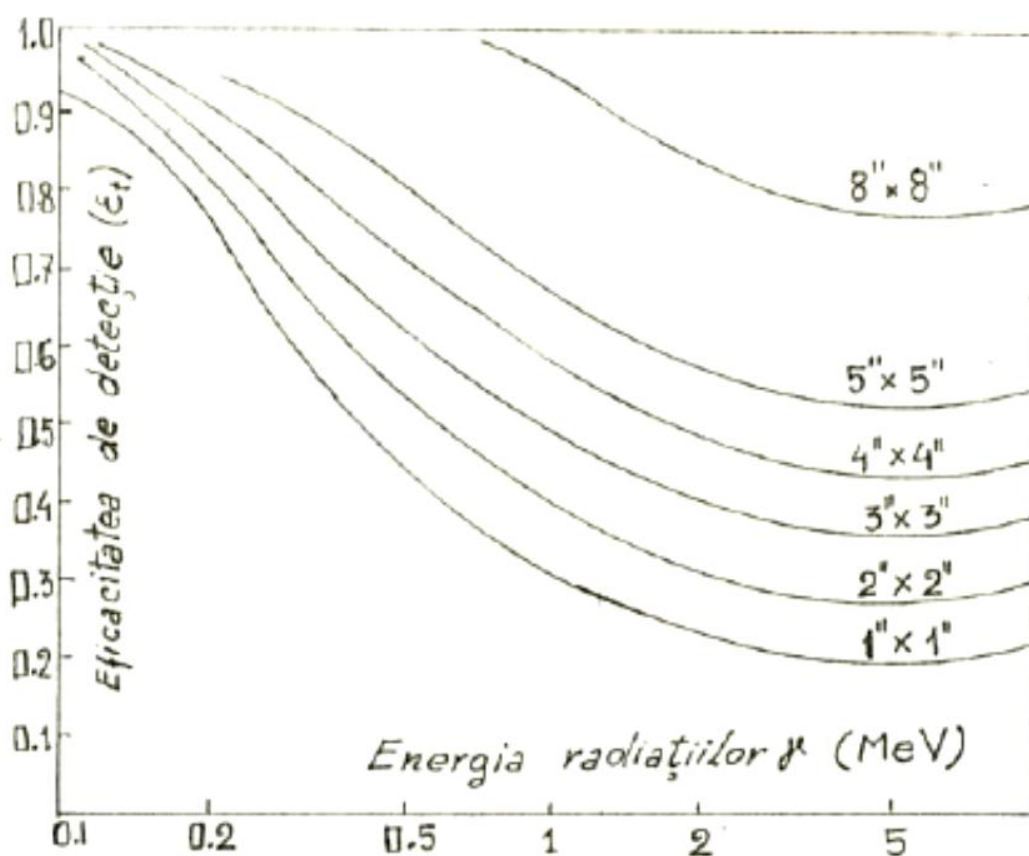
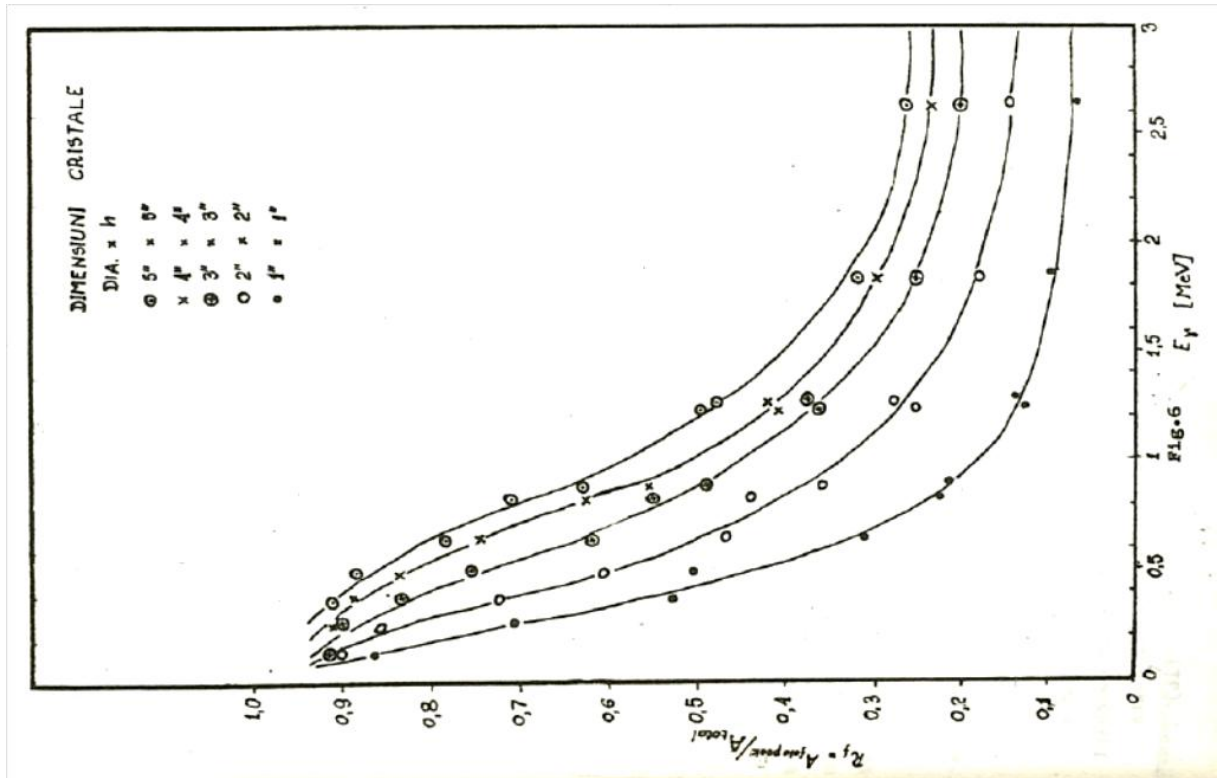


Fig.4 - Eficacitatea de detecție totală pentru cristale NaI(Tl) de diverse dimensiuni, cu sursa la 10 cm de cristal.

a





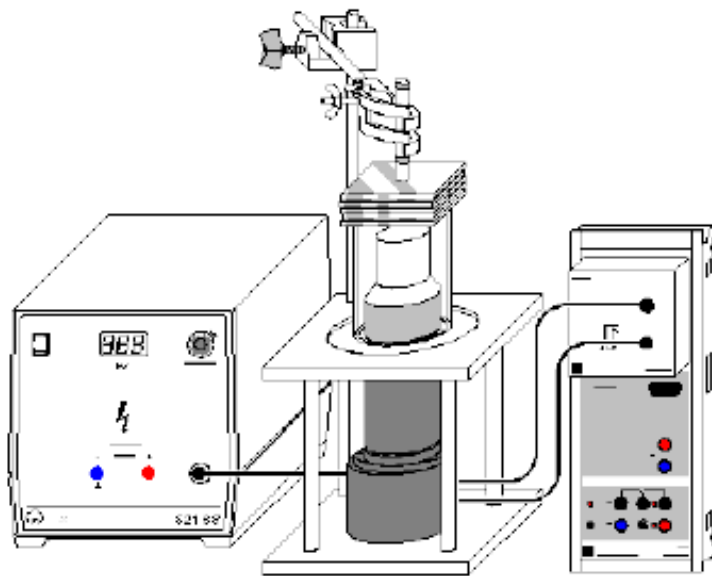
## **5. Gamma and X Rays Attenuation**

## Gamma and X Rays Attenuation

### Part I - Gamma Attenuation

The experimental set-up is presented in figure.

**Absorption of  $\gamma$  radiation**



### Theory and evaluation

The  $\gamma$ -quanta emitted from the radioactive source (Co-60) are absorbed into the different material layer (lead, aluminium, concrete, et others) with a thickness  $d$ , in different ways. The intensity of the radiation beam  $I$  is weakened by the absorption layer as compared with the  $I_0$  value in the air. The radiation beam  $I$  almost decrease exponentially as the thickness of layer  $d$  increases.

$$I = I_0 e^{-\mu d}$$

It follows from this that the half-value thickness  $d$  is determined using the coefficient  $\mu$ :

$$d_H = \frac{\ln 2}{\mu}$$

or

$$\mu = \frac{\ln 2}{d_H}$$

The similar discussion could be done if we consider the counting rate ( $R$ ), because  $I \approx R$ . The attenuation coefficient  $\mu$  characterises the absorption behaviour of the material towards the gamma-quanta.

Layers of matter of a different thickness  $d$  and varying densities are arranged in radiating field between the gamma source Co – 60 and the counter detector. The half value thickness for iron, aluminium, plexiglas and concrete will be determined and the coefficient of weakening will be determined for every material.

The densities of materials are presented in the following table:

Material	Density g/cm <sup>3</sup>
Lead	11.11
Iron	7.68
Aluminium	2.70
Concrete	1.87
Plexiglass®	1.19

The weakening coefficient  $\mu$  increases in an approximate proportion to the density of the absorbing material:

$$\mu = \mu_m \rho$$

The physical argument is the following: the attenuation of X and gamma rays take place predominantly in the electron shell of the absorber atoms.

The absorption coefficient  $\mu$  should be proportional to the number of electrons in the shell per unit volume, or approximately proportional to the density of the material.

Using these materials, determine the absorption coefficients and shows their dependence by density.

## Part II – X-Rays Attenuation

It has been just over a century since the discovery of X rays by Roentgen, and it seems as if every field of science uses X rays and X-ray analysis!

X rays are electromagnetic radiations with wavelengths that are usually longer than gamma wavelengths and energies lower than for gammas.

They originate from transitions among the atomic electrons, where an outer-shell electron fills an electron vacancy in the K shell and the energy change is the x-ray's energy.

A K x ray is not always emitted from such a transition. A competing process, the Auger effect, results in the emission of an atomic electron and no x ray. If a K<sub>shell</sub> vacancy exists, the fractional probability for xray emission is called the fluorescence yield, which increases as the atomic number increases. Moseley, in a series of experiments with K x rays, showed that the periodic array of elements (about 80 years old at the time of his experiments) was an array built on the increasing atomic number (Z) of the nucleus. Moseley used the Bohr atomic model as the basis of his analysis of the x-ray data to prove that both theory and experiment showed that the K x-ray energies are proportional to the square of the atomic number (more precisely, one less than the atomic number. This allowed Moseley to determine the atomic number of an element from a measurement of the energy of its K xrays.

Moseley created K vacancies by bombarding elemental targets with an electron beam. Similar effect could be obtained using photons.

An **X-ray tube** is a vacuum tube that produces X-rays. As with any vacuum tube, there is a cathode, which emits electrons into the vacuum and an anode to collect the electrons, thus establishing a flow of electrical current, known as the beam, through the tube. A high voltage power source is connected across cathode and anode to accelerate the electrons. The X-ray spectrum depends on the anode material and the accelerating voltage. Electrons from the cathode collide with the anode material, usually tungsten, molybdenum or copper, and



accelerate other electrons, ions and nuclei within the anode material. About 1% of the energy generated is emitted/radiated, usually perpendicular to the path of the electron beam, as X-rays. The rest of the energy is released as heat. The X-ray photon-generating effect is generally called the Bremsstrahlung effect and X ray spectrum is continuum, contrary to the mechanism discovered by Mosley where photon spectra is discrete. In the Bremsstrahlung process an accelerated electron (or other charged particle) radiates a photon with an energy in the X-ray range.

Generally X-rays investigations are non – destructive for the sample. In this laboratory work, the investigations are only qualitative.

### **Experiment procedure:**

1. Using different materials: plexiglas, plastic, metal (Al, Pb), investigate qualitatively the absorption of X- rays using the image obtained on the fluorescent screen. Try to correlate this observation with the thickness of the material and compare the results with these obtained using gamma rays (qualitative). What radiations are more penetrating?
2. Is it possible to put in evidence a relation of proportionality between the absorption coefficient and the density of the material?
3. Investigate the minimum dimension of a defect that could be observed on the screen.
4. Are the observed effects sensitive to the distances source – object – screen? Is the geometry of experimental configuration important? Please use a slit for experimental studies.
5. Please identify the hide object using a the image obtained in a radioscopy.

Please comment all obtained results.

## **6. Study of $\alpha$ Particles in Air**

## Study of $\alpha$ Particles in Air

### Theory and evaluation

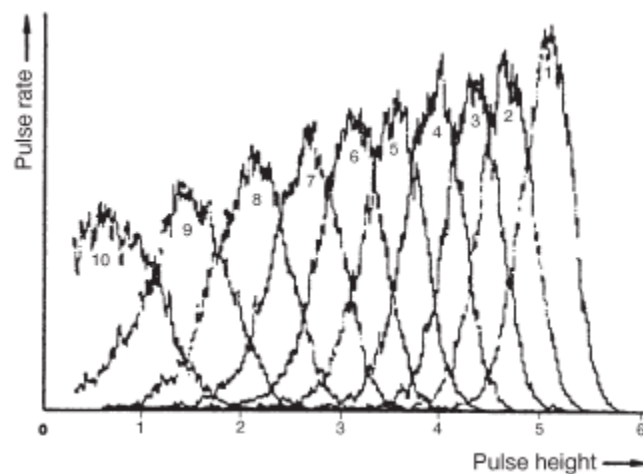
**Alpha decay:** This is the emission of an alpha particle (Helium nucleus) from the nucleus:  $(Z,A) \rightarrow (Z-2,A-4) + \alpha$ . The emitted alpha particles are monoenergetic, their energy in the range of a few MeV. The alpha interacts strongly and has a very short range - a few cm in air.

$\alpha$ -particles undergo various interactions during their passage through material. One possibility is that of scattering on contact with atomic nuclei. These elastic Rutherford scattering processes in which the  $\alpha$ -particles suffer virtually no energy losses are extremely rare in relation to their inelastic interactions with atoms. These inelastic collisions cause ionization of the atoms, i.e.  $\alpha$ -particles lose a small proportion of their energy to an electron in the atomic shell. The mean energy loss per collision in air is 33.7 eV. The frequency of such collisions and in consequence the energy loss per unit of length is a function of the electron density in the absorber material and of the energy of  $\alpha$ -particles. The slower the speed of movement of  $\alpha$ -particles along their path is, the more likely are interactions to occur with shell electrons, giving rise to an increase in the differential energy loss and a decrease in particle energy.

The probability of an electron colliding with  $\alpha$ -particle is proportional to the electron density in the absorbent gas. At identical pressure and temperature values, this electron density in different gases follows the same behaviour pattern as the electron number  $N$  in the gas molecules.  $N$  is equal to the atomic number of the atom in question and, in the case of molecules, to the sum of the atomic numbers of the atoms contained in the molecule.

Figure 1 shows an example of a measurement carried out at different pressure values  $p$ . The individual spectra have been numbered and the corresponding data will be found in the table under these serial numbers. A similar result is obtained if the gas is at a constant pressure but their thickness increase.

The global effect is a decrease of the energy of registered particles, their number and increase of their energetic spread due to multiple interactions up to their detect.



It is to be noted that the differential energy loss of the  $\alpha$ -particle again decreases toward the end of its path as described by the Bethe formula:

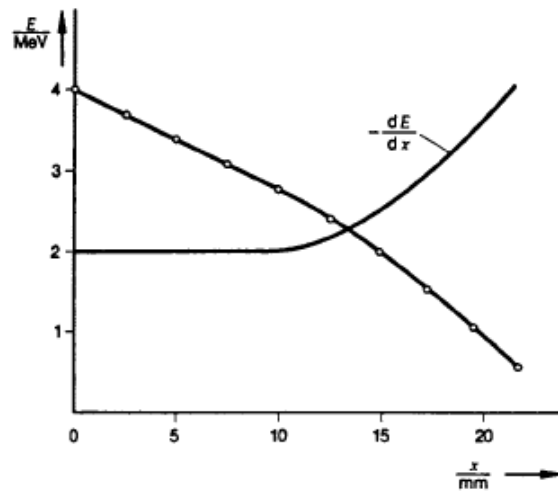
$$\frac{dE}{dx} = -\frac{n Z z^2 e^4}{4\pi \epsilon_0^2 m_0 v_\alpha^2} \cdot \ln \frac{2 m_0 v_\alpha^2}{E},$$

Where:

- $n$  = atomic concentration in the retarding material,
- $Z$  = atomic number of the atoms in the retarding material,
- $z$  = atomic number of the charged particles  
( $z = 2$  for  $\alpha$ -particles),
- $e$  = elementary charge,
- $\epsilon_0$  = electron mass,
- $v_\alpha$  = velocity of the  $\alpha$ -particles,
- $\bar{E}$  = mean ionization potential

In Figure 2 the mean energy and the differential energy loss  $-(dE/dx)$  of  $\alpha$ -particles has been plotted as a function of  $x$ .

Figure 2



This connection between the differential energy loss and  $\alpha$ -particles velocity is shown in diagrammatic form in Fig. 3.

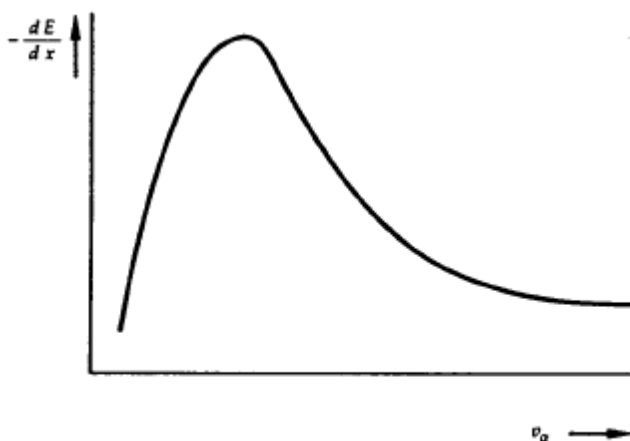


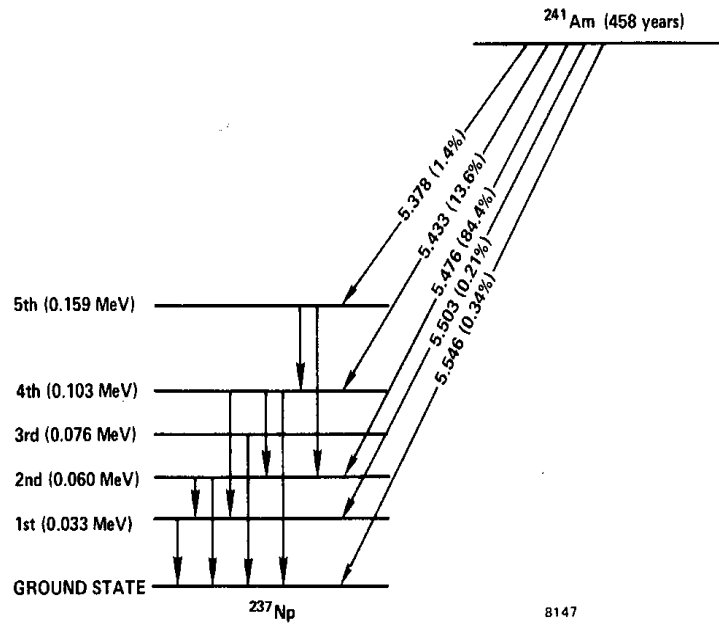
Figure 3

The present experiment provides confirmation of this state of affairs only for the velocity range above the peak of the function shown in Fig. 3. The extremely low velocity range, in which the differential energy loss value again decreases, cannot be recorded with the semiconductor detector as result of the noise produced by the measuring device.

### The alpha particle sources used in the laboratory

#### $^{241}\text{Am}$ source

The spectrum of the  $^{241}\text{Am}$  source (3.7 kBq) is shown in the figure below (Figure 4): energy level diagram (decay diagram), transition probability, excited nuclear states,  $\gamma$  emission, connection between the fine structure of the  $\alpha$ -spectrum and the accompanying  $\gamma$ -spectrum.



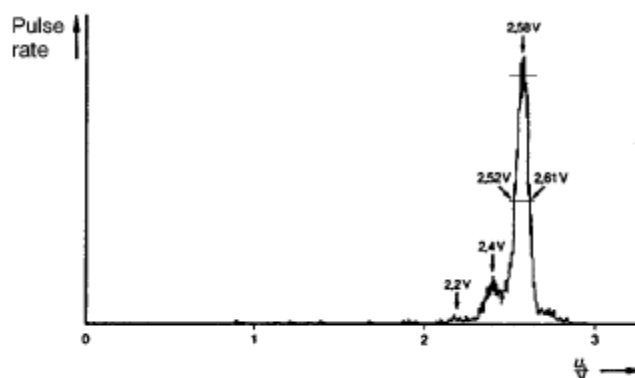
Energy level diagram for the  $\alpha$ -decay of  $^{241}\text{Am}$ .

B147

Five different transition possibilities are apparent from the basic state of the  $^{241}\text{Am}$  into different excited states of the  $^{237}\text{Np}$  isotope. The energy differences are sufficiently great for the resolution capacity of the measuring equipment to ensure separation of the anticipated five emission lines. It is however evident from the transition probabilities given in the table that detection of  $\alpha$ -transitions 4 and 5 may give rise to problems.

Transition No.	$E_{\alpha}$ (value from the literature)	Transition probability (%)
1	5.389	1.3
2	5.443	12.7
3	5.486	86
4	5.513	0.12
5	5.545	0.25

The measured spectrum (optimized) is indicated in the figure below.



The known value of 5.486 MeV has been assumed in this case for the  $\alpha$  - energy of line 3 (the principal peak).

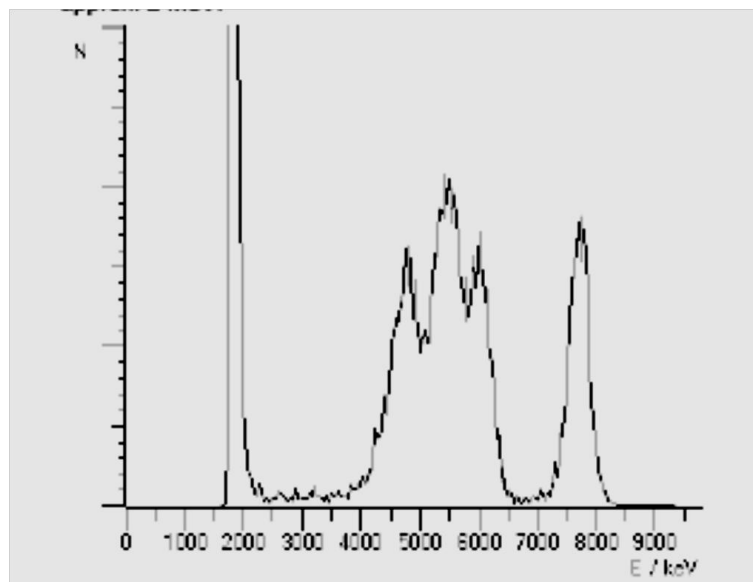
The two peaks 1 and 2 preceding the principal peak are clearly apparent. A slight shoulder at the bottom of the height-energy arm of the principal peak is also apparent.

### $^{226}\text{Ra}$ source

Each  $^{226}\text{Ra}$  source contains the following nuclides in the uranium-radium decay series (disregarding nuclides such as  $^{218}\text{At}$ ,  $^{218}\text{Rn}$ ,  $^{210}\text{Tl}$  and  $^{206}\text{Tl}$  which only occur with very low activities):

Nuclide	Type of decay	$\alpha$ -energy MeV
Radium-226	$\alpha$	4.78
Radon-222	$\alpha$	5.48
Polonium-218	$\alpha$	6.00
Lead-214	$\beta^-$	-
Bismuth-214	$\beta^-$	-
Polonium-214	$\alpha$	7.68
Lead-210	$\beta^-$	-
Bismuth-210	$\beta^-$	-
Polonium-210	$\alpha$	5.30
Lead-206	Stable	-

With the exception of radon-222 and polonium-210 these energies are so widely separated that they can be easily resolved for a covered source.



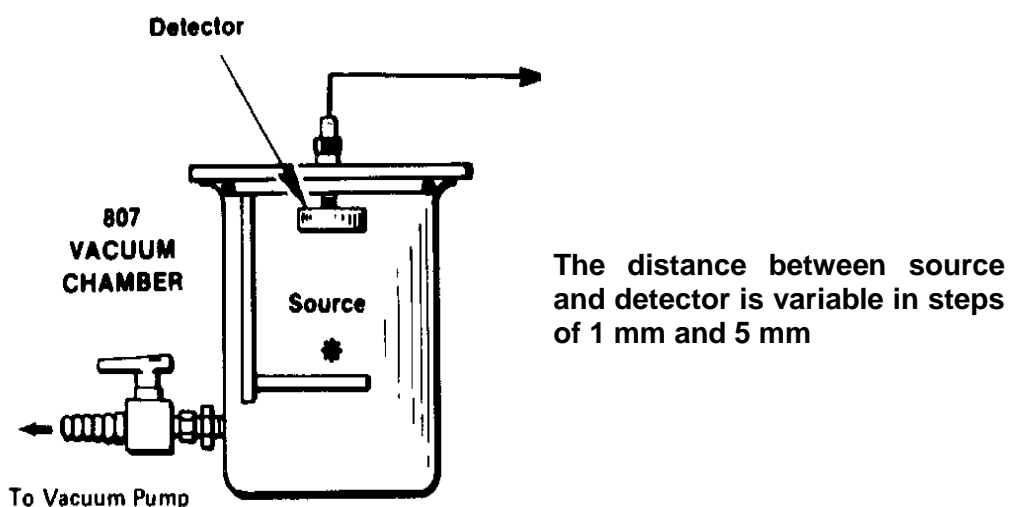
## Experimental set up

The detector used in this experiment is Passivated Implanted Planar Silicon (PIPS) Detector. This is a product of modern semiconductor technology. In most applications, this detector replaces silicon surface barrier (SSB) detectors and diffused junction (DJ) detectors, both of which are still made the same way they were made in 1960.

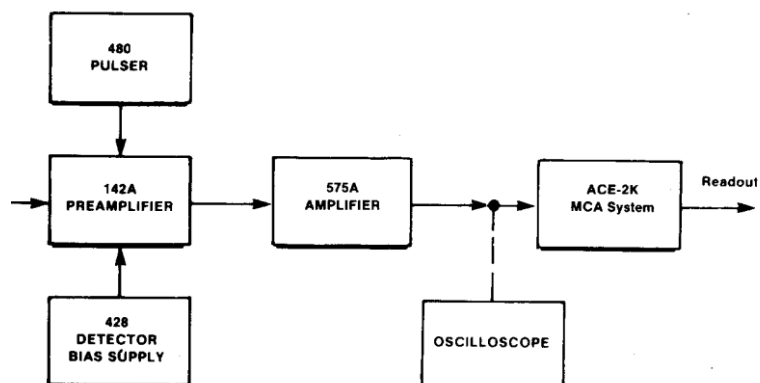
The PIPS detector has a number of advantages over older types:

1. All junction edges are buried.
2. Contacts are ion-implanted to form precise, thin, abrupt junctions for good alpha resolution.
3. Entrance window is stable and rugged – it can be cleaned readily and reliably.
4. Very low leakage current.
5. Dead layer (window) thickness is less than that of comparable SDB or DJ detectors.
6. Standard detectors are bakeable to 100 °C .

The detector is coupled at a reaction chamber.



The signal obtained is amplified and analysed in a standard system for alpha spectroscopy with emulated Multi Channel Analyzer. MAESTRO is a multichannel analyzer (MCA) “emulation” software package.



## Tasks



1. The pulse height corresponding to the every peak value (H) of the lines is proportional with the  $\alpha$ -energy minus the energy loss in the source, in the window of the detector and in the gas between source and detector ( $\Delta E$ ). This quantity cannot be measured in the experiment.
2. Please realize the calibration of the system using  $^{226}\text{Ra}$  source.
3. Using  $^{226}\text{Ra}$  source please investigate the interaction of alpha particles in air. Change the distance source detector in steps of 1 mm and finally in steps of 5 mm.

$\Delta x$ [mm]	$E_1 = 7.68$ MeV	$E_2 = 6.00$ MeV	$E_3 = 5.48$ MeV	$E_4 = 5.30$ MeV	$E_5 = 4.78$ MeV

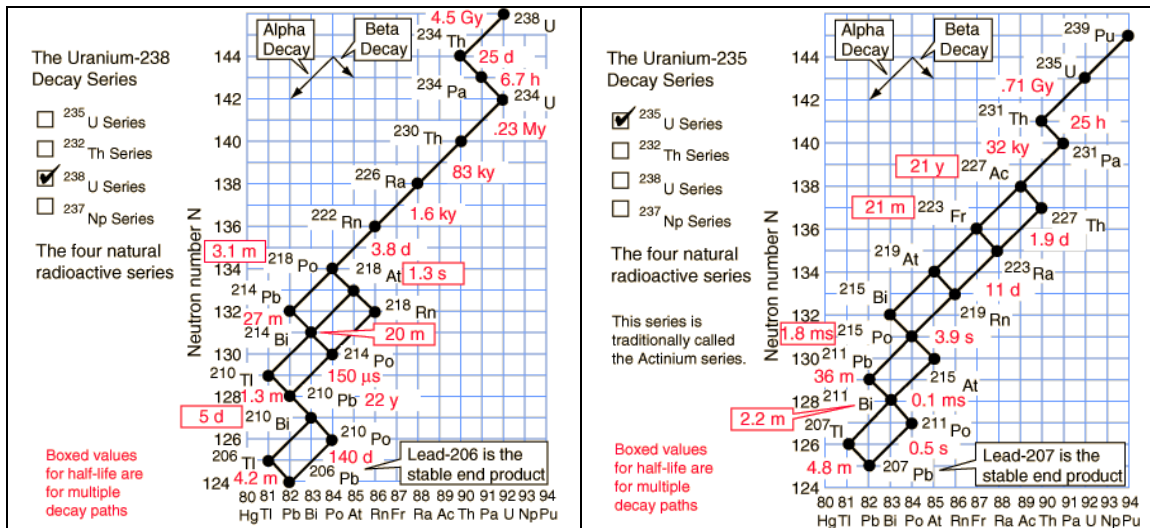
4. Plot Energy (in MeV) versus distance (in mm) for all energies of  $^{226}\text{Ra}$  source. Fit this curve.
5. Using this experimental result plot  $\Delta E / \Delta x$  versus E considering  $\Delta x = 2$  mm.
3. Using the  $^{241}\text{Am}$  source identifier the energies of their spectra

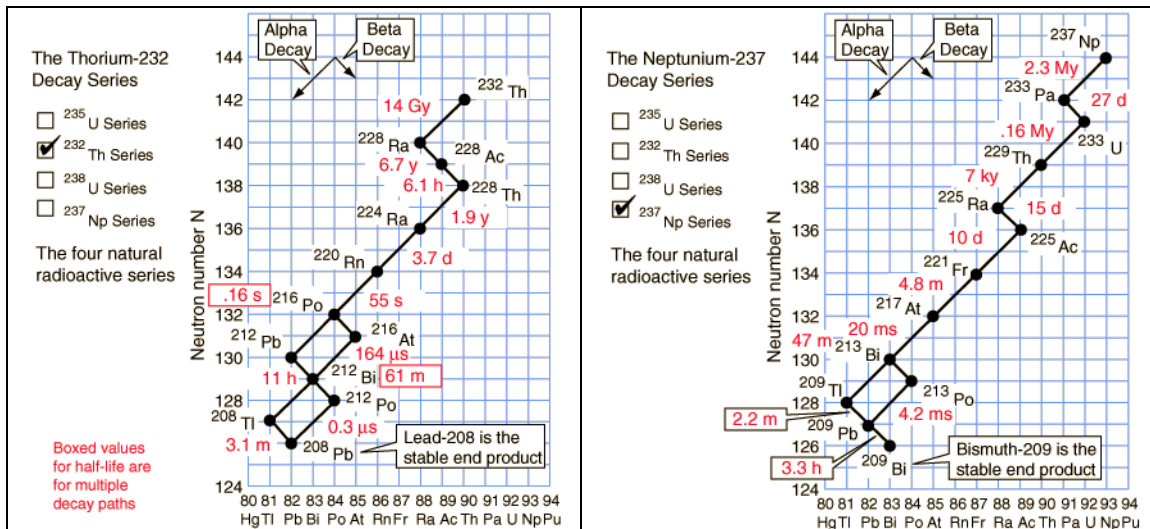
**Annexe**

**1. Radioactive decay series:** 3 - naturals and 1 – artificial (The members of this series are not presently found in nature because the half-life of the longest lived isotope in the series is short compared to the age of the earth).

Units:

$1\mu\text{s} = 10^{-6}\text{s}$ ,  $1\text{ms} = 10^{-3}\text{s}$ ,  $1\text{My} = 10^6\text{y}$ ,  $1\text{Gy} = 10^9\text{y}$





## **7. Beta Backscattering as a function of Atomic Number**

## Beta Backscattering as a function of Atomic Number

### Objective

The student will investigate the relationship between

- a) absorber thickness and backscattering
- b) absorber material (atomic number) and backscattering.

### Backscattering Theory and its Applications

A  $\beta$  particle entering a material can be deflected when it interacts with the nuclei of the material. The  $\beta$  particles are oppositely charged to the positively charged nucleus and thus an attractive force exists between the two. The deflections that result are dependent on the initial energy of the  $\beta$  particles but the effect is of a general scattering of the particles. This usually has the effect of changing the forward direction of a  $\beta$  particle by a few degrees, but occasionally if the  $\beta$  particle is suitably orientated in relation to the nucleus, the  $\beta$  will be deflected with an angle value around 180 degrees and the  $\beta$  particle exit the material from the same side as it entered. It is this phenomenon that is known as backscattering.

The processes by which  $\beta$  particles lose energy in absorbers are similar to those for alphas. However, an additional process must be considered in dealing with  $\beta$  absorption. This is the process whereby electromagnetic radiation (with continuum spectra), called bremsstrahlung, is produced.

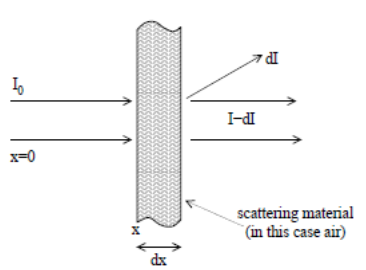
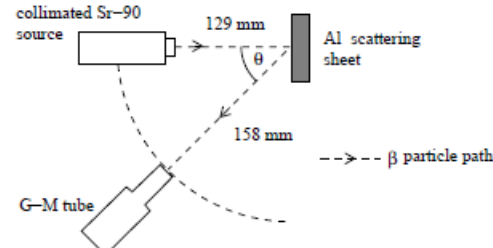
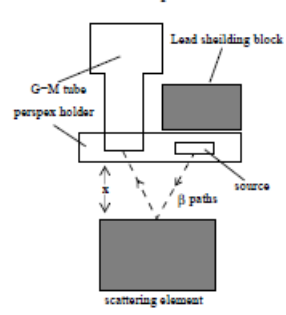
A  $\beta$  particle has a very small mass and one – half the value of the charge on an  $\alpha$  particle. So, for a given energy, a  $\beta$  particle will have a much greater velocity than an  $\alpha$  particle. As a result of these and other factors, the  $\beta$  particle has a lower specific ionization which means that its penetration in any absorber will be much greater than that of an  $\alpha$  particle.

For thick samples, there are not yet theoretical relationship on  $\beta$  particle backscattering due to the complexities of calculations involving multiple scattering. That is to say when a  $\beta$  particle enters a material it may scatter many different atoms before leaving the material and thus the idea of backscattering being uniquely an interaction between one  $\beta$  particle and one atom breaks down. In certain cases relationships developed to deal with single scattering can be used as a possible approximation to what is actually happening.

In any case the relationships that do exist concerning backscattering are purely empirical.

Beta particle backscattering has been a subject for investigation for many years; yet data, theoretical or experimental, on any relationships between atomic number ( $Z$  number) of the scatterer, the angle of scattering and the count rate, are sparse. The subject has been mainly of interest to physicists involved in the laws of charged particle scattering and those developing devices such as  $\beta$  ray thickness gauges. The recent increase in the availability and use of high-energy electron accelerators has caused a necessity for greater understanding of the above ideas. Specific examples of the applications are in the use of radiation therapy for the treatment of tumours. This is due to the fact that the density of tissue is far from even throughout the human body and at high/low density boundaries  $\beta$  ray backscattering becomes a significant factor in determining the absorbed dose of the surrounding tissues.

## Geometries for scattering processes.

Geometries for scattering processes	
Transmission detection	Backscattering detection
 <p style="text-align: center;"> <math>-dI \propto I dx \Rightarrow cI = e^{-\mu x},</math>  <math>I = I_0 \text{ at } x = 0 \Rightarrow c = 1/I_0,</math>  <math>I = I_0 e^{-\mu x}.</math> </p>	 <p style="text-align: center;">Top View</p> 

A simplified formula for the backscattering of mono-energetic electrons was given by Bethe et al. in the form:  $R \propto (c + \cos \vartheta) \cos \vartheta$ , where  $\vartheta$  is the scattering angle and  $c$  is a numerical constant. For continuous  $\beta$  ray spectrum the results are more complicated.

### Atomic Number Dependence

As it has already been suggested there is a connection between the atomic number ( $Z$  number) of an element and its ability to produce high  $\beta$  backscatter count rates. An empirical dependence was given:  $R = k_1 Z^n + k_2$ , where  $k_1, k_2$  are two constants that must be determined using experimental data and  $n$  lies between 0.32 to 0.5.

For compounds and molecules, the following equations could be considered:

$$\bar{Z} = \sum_i C_i Z_i$$

where

$$C_i = \frac{n_i A_i}{M}$$

Here  $n_i$  is the number of atoms by type "i" in the compound, their atomic mass  $A_i$  and  $M$  – the mass of the molecule.

### Expected results

As the thickness is increased, more and more number of atoms (scattering centers) are available and hence back scattering grows in intensity. But the range of  $\beta$  particles sets a limit to the increase of back scattering, which becomes constant below a certain thickness called saturation or critical thickness. Theoretically for normal collisions the thickness should be equal to half the range " $S_R$ " of the  $\beta$  particles. Since collisions occur in all possible obliquities, the maximum back scattering is obtained for a thickness equal to  $0.2 S_R$ .

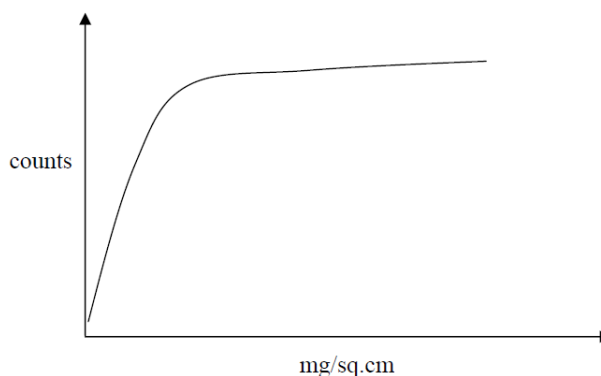
As the atomic number  $Z$  of the material increases, the number of positive charges in the nucleus and the electron density increases gradually. Thus an increase in the back scattering intensity as  $Z^n$  is justified.

Tabulate the thickness and corresponding count rate as shown below.

$$R_t = R_s[1 - e^{-t(\mu + \mu')}]$$

where  $t$  is the thickness of the measured sample, with  $t_s$  the saturation thickness;  $R_t$  is the count rate with backing material of thickness  $t$ ;  $R_s$  is the count rate with material of thickness  $t_s$ ;  $\mu$  is the absorption coefficient of back scattering  $\beta$  particles and  $\mu'$  is the absorption coefficient of back scattered rays.

Typical result is presented in the figure below



Usual range of thickness that can be measured by using  $^{90}\text{Sr} / ^{90}\text{Y}$  is 30 to 150 mg/cm<sup>2</sup> since  $\beta$  back scattering depends upon the thickness and the atomic number of the backing material by keeping the atomic number constant, i.e., by taking all the samples made of the same material (e.g. Aluminum), the effect of atomic number on the back scattering intensity can be kept constant. Thus scattering intensity depends only on the thickness of the back scattering material.

### Experimental Procedure:

1. Connect the back scattering setup to the counter system.
2. Place the material foil at a suitable distance above the source using the holder.
3. Take a time of the measure as a relative error to be below 5%.
4. Repeat the counting five times and find out the average counting rate.
5. Repeat the procedure for all the known foils as well as the unknown foil.

Distance between the back scattering surface and the detector is very sensitive parameter. If the detector presents almost  $2\pi$  geometry to the incoming back scattering radiation being very close to the scatter surface, this improves the efficiency further.

### Observation & Results:

Tabulate the thickness and corresponding count rate as shown below.

Thickness	Counts					
	1	2	3	4	5	average

Plot the graph of thickness ( $\text{mg}/\text{cm}^2$ ) versus average count rate and from the graph find out the thickness of the unknown foil. Measure the actual thickness of the foil using a micrometer and find out the percentage error in the thickness measurement using  $\beta$  back scattering technique.

Thickness of the foil (experimental) =  $\text{mg}/\text{cm}^2$

Thickness of the foil (Measured) =  $\text{mg}/\text{cm}^2$

Percentage error = .....

Using his plot find the unknown thickness of a foil. Compare with the measured value using the micrometer.

## **8. Absorption of beta particles in different materials**



# Absorption of beta particles in different materials

## 1. Introduction

Transmission of electrons and positrons through different materials has been widely studied in the past and the range of the particles in different materials was been investigated as a function of particle energy and the atomic number of the material. Systematic measurements, carried out for several chemical elements and for different electron energies, allowed to extract semiempirical relations useful to parametrize their range in any material with  $Z = 1$  to  $Z = 92$ , in the energy interval between 0.3 keV and 30 MeV. Theoretical compilations of mono-energetic electron and positron ranges in various materials have also been reported in different publication. In the case of continuous spectra, as it is the case for electrons from a radioactive beta source, a semiempirical relationship between the mass absorption coefficient and the maximum electron energy exists also, following a set of measurements performed using electrons from several radioactive sources traversing different materials. A theoretical discussion of the mass absorption coefficients has been given in literature.

## 2. The experimental setup and measurements

**Safety Note:** The radioactive sources used in this experiment are extremely weak and therefore can be handled without any danger of overexposure to radiation. However, it is always prudent not to handle any radioactive source more than is necessary.

### 2.1 The experimental setup

The experimental setup used for the measurements discussed in the present paper basically includes a Geiger counter or a detector with scintillations, connected to a control box, which serves both to power the counter and to record the counts in a given time interval, a mechanical structure to hold the radioactive source in front of the counter and a variable set of absorbers placed between the source and the detector.

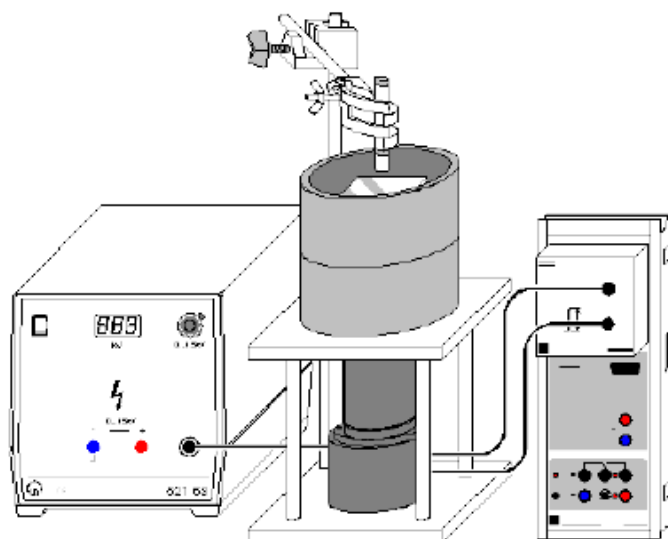


**Figure 1** Experimental setup

The number of particles entering through the window of the detector per unit of time  $\Delta I$ , is proportional to the counting rate indicated by the detector. If  $\Delta I_0$  is the number of particles entering the counter detector per unit time in the absence of absorbing material, in the presence of the

absorbing material of thickness  $d$ , we expect to have, with  $\Delta I$  as the number of particles entering the counter tube per unit time

$$\Delta I = \Delta I_0 e^{-\mu d} \quad (1)$$

where  $\mu$  is the attenuation coefficient. The last equation could be used as:

$$\mu = \frac{\ln\left(\frac{\Delta I_0}{\Delta I}\right)}{d} \quad (2)$$

Plotting  $\Delta I$  semi logarithmically versus  $d$  makes it possible to measure the attenuation coefficient of the different materials used.

In Fig. 3 the counting rates plotted semi logarithmically versus  $d$  is presented as example. The graph consists of straight lines which prove the validity of Eq. (1).

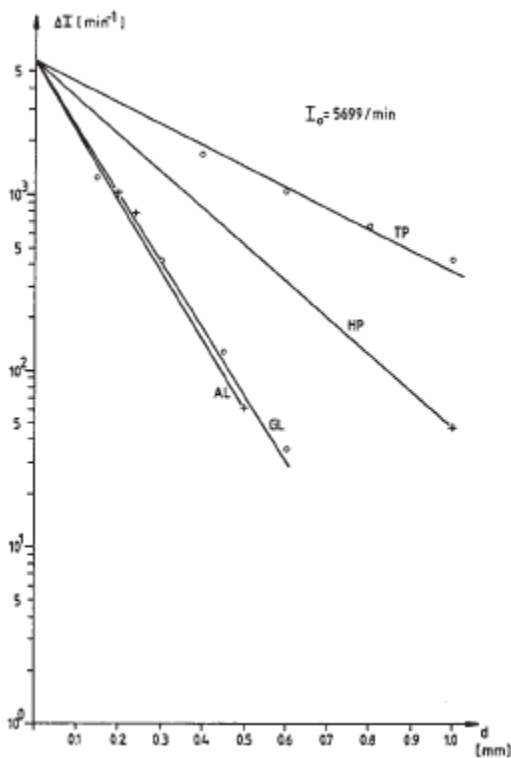


**Figure 2.** Counting rates (plotted as logarithmically axis) versus  $d$

From the slope of the straight lines in Figure, the attenuation coefficients can be calculated using Eq. (2).

The figure (bellow) shows the attenuation coefficient as a function of the density. The proportionality between  $\mu$  and  $\rho$  (density) is the mass attenuation coefficient  $\mu_m$ .

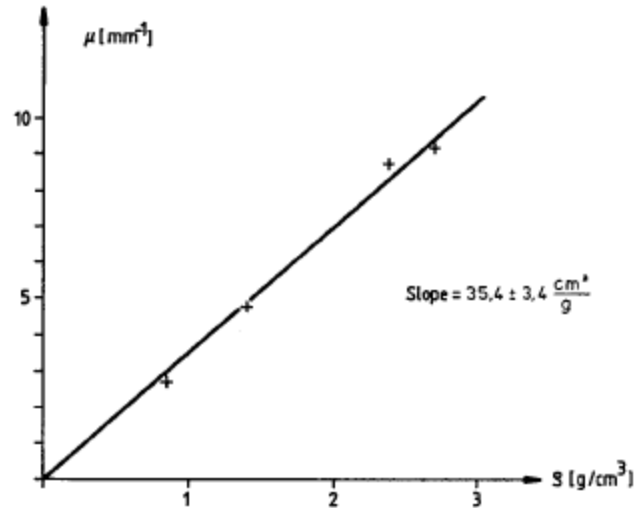


**Figure 3.** The attenuation coefficient as a function of the density

$$\mu_m = \frac{\mu}{\rho}$$

For a particular energy distribution of the particles considered, e. g. for particular  $\beta^-$  emitting source,  $\mu_m$  is a constant for all absorbing materials. The quantity  $\mu_m$  can be calculated using the empirical formula:

$$\mu_m = \frac{22 \frac{\text{cm}^2}{\text{g}}}{W_m^{1.333} [\text{MeV}]} W_m$$

(if the maximum energy of the particles,  $W_m$ , is  $W_m > 0.5 \text{ MeV}$ ).

## 2.2 The radioactive beta sources

a) The  $^{90}\text{Sr}/^{90}\text{Y}$  is beta source. The  $^{90}\text{Sr}$  source is a beta emitter, with a half-life of 28.8 years, decaying into  $^{90}\text{Y}$  with an end-point energy of 0.546 MeV.  $^{90}\text{Y}$  is also a beta emitter, with a half-life of 64 h and an end-point of about 2.3 MeV. Due to the half-lives of the two isotopes, a secular equilibrium between the two decay processes is reached, with a continuous beta spectrum that extends up to 2.3 MeV and has two components associated with the two isotopes. The detailed shape of the continuous energy spectrum is indicated in the figure 1, that was modelled in the GEANT simulations by the use of the Fermi theory of the beta decay.

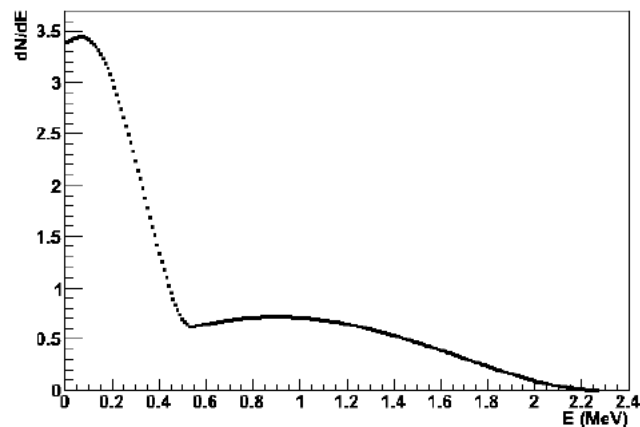


**Figure 4.** Energy spectrum of the electrons emitted from the  $^{90}\text{Sr}/^{90}\text{Y}$  source, as modelled in the GEANT simulation.

b) Thallium 204 beta decays to Lead 204 (branching ratio 98%) with a half-life of 3.9 years. The maximum of the beta energy is 0.766 MeV.

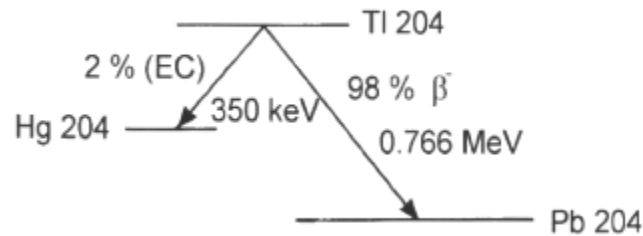


**Figure 5.** Thallium 204 beta decays

### 2.3 Measurements

a) Using  $^{90}\text{Sr}/^{90}\text{Y}$  beta source it is possible to measure the attenuation coefficient of the different materials used. The foils of different materials exist in laboratory and the supervisor will suggest you the optimal choice.

The counting rate without an absorbing material will be measured at a distance of the order of 25 - 35 mm between source and detector.

In the fixed geometry the foils will be placed in front of detector.

Plotting  $\Delta I$  semi logarithmically versus  $d$  makes it possible to measure the attenuation coefficient of the different materials used.

Plot the curve:  $\mu = f(\rho)$  and compare the results with the empirical equation.

The thickness of the foils will be measured using the micrometric ruler from laboratory.

b) Attenuation of betas in aluminium using  $^{204}\text{Tl}$  source and determine the range of electrons.

The range of the most energetic of the decay electrons can be determined by placing aluminium foil absorbers between the source and detector. A typical absorption curve is shown in Figure 7.

The maximum range  $r$  is the point where the absorption curve meets the background.

You should start by making a careful measurement of background, and you should repeat this measurement with one, two, three,....., foils of aluminium up to obtain a value of counter rate close by background.

The typical result is:

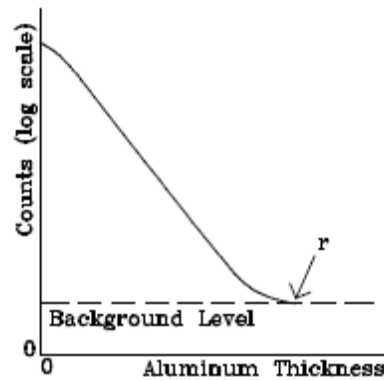


**Figure 6.** Determination of range of electrons in aluminium

In this experiment, therefore, we will use an *approximate* empirical relationship between range and energy for low energy electrons:

$$r = \frac{0.412 \left[ \frac{g}{cm^2} \right]}{\rho} (E)^{1.29}$$

where  $r$  is in cm,  $E$  is in MeV, and  $\rho$  is the density of the stopping material in  $g/cm^3$ . Note that the density of Aluminum is  $2.702 g/cm^3$ .

(L. Katz and A. S. Penfold, "Range-Energy Relations for Electrons and the Determination of Beta-Ray End-Point Energies by Absorption," *Revs. Modern Phys.* **24**, 1 (1952).)

Compare experimental result with the empirical equation for range of electrons in aluminium.

Suggestions for experimental set-up:

- The voltage for scintillator detector: 600 V
- Set the MCA with the following parameters: 256 channels, 100 seconds for all measurements using  $^{90}\text{Sr}/^{90}\text{Y}$  source and 400 second for  $^{204}\text{Tl}$  source.
- Because the beta spectra are continuous, in the experimental data integrated values of the spectra must be used; for example an adequate region is between channels 100 and 250.